universität wien

MASTERARBEIT

Titel der Masterarbeit

„ Characterization of antibodies recognizing the alpha 5 subunit of nicotinic acetylcholine receptors “

verfasst von

Christoph Zlabinger, BSc

angestrebter akademischer Grad

Master of Science (MSc)

Wien, 2015

Studienkennzahl lt. Studienblatt:	A 066834
Studienrichtung lt. Studienblatt:	Masterstudium Molekulare Biologie
Betreut von:	Mag. Dr. Petra Scholze, Privatdoz.

Danksagung

Ich möchte an erster Stelle meine Eltern meinen Dank und Anerkennung aussprechen, da sie mich in all meinen Entscheidungen unterstützt, aber niemals in eine Richtung gedrängt haben.

Petra Scholze für die gute Zusammenarbeit und die wichtigen Lektionen um integre Wissenschaft zu betreiben.

Sigismund Huck und die Labor - “Damen“ Traude, Gabi und Karin für die gute Unterstützung und die freundliche Arbeitsumgebung.

Table of Contents

Abstract

The nicotinic acetylcholine recptor (nAChR) is a pentameric ligand-gated ion channel. It plays a key role in the central nervous system (CNS) as well as in the peripheral nervous system (PNS) and even in non-neuronal tissue. The receptor is assembled by a subset of nine alpha-units (α2-α10) and three beta-units (β2-β4) and therefore grants a wide variability of receptor subtype combinations. The α5 subunit in particular is an accessory subunit and alters the pharmacological and biophysical properties of its receptor. Studies show the involvement of α5 in nicotine addiction, lung cancer, attention circuitry and pain, proving that further knowledge about this nAChR subunit is of importance.

Our aim was to generate subunit specific antibodies against the α5 nAChR subunit, capable of performing in Immunoprecipitation, Immunohistochemical and Immunocytochemical staining methods. Additionally with specific antibodies against α2, α3, α4, α5, α6, β2 and β4 subunits, the nAChR subunit composition of wild-type, α5-knockout, β2-knockout and β4-knockout mouse interpeduncular nucleus (IPN) should be revealed.

We immunized two rabbits (S23a and S24a) as well as four guinea-pigs (S35, S36, S37 and S38) with a fusion-protein carrying an α5 sequence originally located at the intracellular loop between M3 and M4 transmembrane-domains of the nAChR subunit. The generated antibodies in the blood of these animals were then purified using affinity columns and subjected to rigorous tests. Immunoprecipitations were conducted in heterologous tissue (transfected HEK-293 cells) and native tissue (Superior cervical ganglion (SCG) and Interpeduncular nucleus (IPN) of wild-type and α5-knockout mice). Immunocytochemical and immunohistochemical stainings were also done in heterologous tissue (transfected HEK-293 cells) and native tissue (Primary neurons of the superior cervical ganglion (SCG) and cryoslices of the median habenula of wild-type and α5-knockout mice). As a reference the former established α5 antibody S23 by Reinhard David 2011 was used.

In heterologous tissue both techniques Immunoprecipitation and Immunocytochemistry yield specific and quantitatively correct results. However in native tissue Immunoprecipitation proved high specificity of the antibodies but the precipitated receptor amount was only 30-50% of the reference antibody. In Immunocytochemical and Immunocytochemical studies only heterologous tissue could be stained specifically.

Additionally using the previously generated and excellently working antibody α5S23 the wild-type mouse IPN nAChR-subunit composition with focus on α5 containing receptors was successfully identified: α2

39.15 ± 3.18 fmol/mg lysate protein; α3 174.16 ± 17.35 fmol/mg lysate protein; α4 139.40 ± 8.40 fmol/mg lysate protein; α5 30.57 ± 1.32 fmol/mg lysate protein; α6 9.84 ± 0.58 fmol/mg lysate protein; β2 183.87 ± 13.20 fmol/mg lysate protein; β4 161.37 ± 21.77 fmol/mg lysate protein.

With the investigation of subunit changes in α5, β2 and β4-knockout tissue we could conclude with the presumption of no compensation mechanisms, that α2, α4, α5 and α6 co-assemble with β2 and α3 co-assembles with β4.

Zusammenfassung

Der nikotinische Acetylcholinrezeptor (nAChR) ist ein pentamerischer ligand-gebundener Ionenkanal. Er spielt eine Schlüsselrolle im zentralen (ZNS), im peripheren Nervensystem (PNS) sowie auch in nicht-neuronalem Gewebe. Der Rezeptor setzt sich aus neun Alpha-Untereinheiten (α2-α10) und drei Beta-Untereinheiten (β2-β4) zusammen, die die Grundlage der großen Kombinationsvielfalt von Untereinheiten im nAChR bilden. Die α5 – Untereinheit ist eine akzessorische Untereinheit und beeinflusst die pharmakologischen und biophysikalischen Eigenschaften ihres Rezeptors. Studien konnten zeigen, dass α5 eine Rolle in Nikotinabhängigkeit, Lungenkrebs, Aufmerksamkeit und Schmerz spielt und daher weitere Untersuchungen dieser speziellen Untereinheit unerlässlich sind.

Unser Ziel war es daher, spezifische Antikörper gegen die α5-Untereinheit herzustellen, die in Immunopräzipitation und Immunzytologischen Methoden anwendbar sind. Zusätzlich wurde mit spezifischen Antikörpern gegen α2, α3, α4, α5, α6, β2 und β4 die Untereinheit-Zusammensetzung von nAChRs im Interpeduncular nucleus (IPN) von wild-typ, β2-knockout and β4-knockout Mäusen bestimmt.

Unsere Gruppe immunisierte zwei Hasen (S23a und S24a), sowie vier Meerschweinchen (S35, S36, S37 und S38) mit einem Fusionsprotein, das ein α5 Sequenzepitop trägt, das aus der intrazellulären Schleifenregion zwischen den Transmembranregionen M3 und M4 der Untereinheit stammt. Das Blut dieser Tiere wurde mit der Hilfe von Affinitätschromatographie-Säulen aufgereinigt und die erhaltenen Antikörper rigorosen Tests unterzogen. Immunopräzipitationen in heterologem (transfizierten HEK-293 Zellen) und nativem Gewebe (Superior Cervical Ganglion (SCG) und Interpedunkular Nukleus (IPN) aus α5-knockout Mäusen) wurden durchgeführt. Immunohistochemische und Immunozytochemische Färbemethoden wurden ebenso in heterologem Gewebe (transfizierten HEK-293 Zellen) und nativem Gewebe (Primärneuronen des SCG und Kryoschnitte der medialen Habenula aus α5-knockout Mäusen) durchgeführt. Als Referenzkontrolle diente der gut charakterisierte Antikörper α5S23, der von Reinhard David 2011 etabliert wurde.

In heterologem Gewebe ergaben sowohl Immunopräzipitationen als auch die Färbungen spezifische und quantitativ korrekte Ergebnisse. In nativem Gewebe hingegen ergaben die Immunopräzipitationen, obwohl sie spezifisch waren, nur 30-50% der Referenzwerte. Die Immunozytochemischen und Immunohistochemischen Färbungen zeigten im heterologen Gewebe spezifisches Signal; im nativen Gewebe allerdings war keine spezifische Färbung möglich.

Die Rezeptorzusammensetzung des IPNs in der Maus wurde mithilfe des gut charakterisierten a5S23 Antikörpers untersucht: α2 39.15 ± 3.18 fmol/mg Proteinlysat; α3 174.16 ± 17.35 fmol/mg Proteinlysat; α4 139.40 ± 8.40 fmol/mg Proteinlysat; α5 30.57 ± 1.32 fmol/mg Proteinlysat; α6 9.84 ± 0.58 fmol/mg Proteinlysat; β2 183.87 ± 13.20 fmol/mg Proteinlysat; β4 161.37 ± 21.77 fmol/mg Proteinlysat.

Mithilfe der α5, β2 und β4-Knockout Geweben konnten wir Rückschlüsse auf die Koassemblierung der Rezeptoren ziehen, unter der Annahme , dass keine Kompensationsmechanismen für Knockout Untereinheiten stattfinden. Unter diesen Vorraussetzungen sahen wir, dass α2, α4, α5 und α6 mit β2, und α3 mit β4 koassemblieren wenn sie einen Rezeptor bilden.

1 Introduction

The cholinergic system is a phylogenetically very old nervous pathway. It plays a key role in higher vertebrates in both, the central nervous system (CNS) and the peripheral nervous system (PNS) as well as non-neuronal tissue (Wessler *et al.*, 1999; Gotti & Clementi, 2004). The key component of the cholinergic system is the nicotinic acetylcholine receptor (nAChR), an ionotropic receptor with its main agonist being nicotine, an alkaloid from plants of the nightshade family and its main antagonist tubocurarine, the effective substance of the commonly known Curare, an arrow poison mixture.

The acetylcholine receptor consists of two distinct families: the former mentioned nicotinic (nAChR) and the muscarinic acetylcholine receptor (mAChR). The muscarinic AChR is activated by the agonist muscarine, the toxin from *Amanita muscaria* commonly known as Fly Agaric and its main antagonist Atropine, the toxin from *Atropa Belladonna*, commonly known as Deadly Nightshade. It is a G-protein coupled metabotropic receptor with relative slow activation times (milliseconds to seconds) in comparison to nicotinic acetylcholine receptors (Albuquerque *et al.*, 2009).

Radioligand binding studies revealed that the nAChR can further be classified in 2 receptor classes. One receptor binding preferably to α-bungarotoxin (α-Bgtx-nAChRs) with µM affinity over nicotine and its agonists with nM affinity. The other receptor type binds nicotine and its agonist with nM affinity but not α-Bungarotoxin. α-Bungarotoxin is a neurotoxin from the venom of the Southeast Asian banded krait, *Bungarus multicinctus*, which irreversibly blocks nAChRs at the acetylcholine binding sites in a competitive action (Chang & Lee, 1963; Lukas & Bencherif, 1992; Young *et al.*, 2003; Gotti & Clementi, 2004).

Moreover the nicotinic acetylcholine receptors can be grouped in neuronal specific and muscle specific subtypes whereas the following work will only focus on the neuronal type AChR.

1.1 Structure

nAChRs belongs like GABA, glycine and 5-HT_3 receptors to the superfamily of cys-loop ion channel receptors and consist of an assembly of 5 subunits around an axis of symmetry creating an ionic pore in the center. The first to adduce visual evidence of its pentameric structure was Cartaud et al by using electron microscopy on membrane tissue of *Torpedo* and *Electrophorus* which are very rich in nicotinic receptor molecules. Further technological and methodical advances using x-ray based crystallography and electron microscopy combined with strong computational simulations led to a stepwise refinement of the known nAChR structure (see Fig. 1) (Cartaud *et al.*, 1973; Toyoshima & Unwin, 1988; Unwin, 1998; Miyazawa *et al.*, 2003; Unwin, 2005).

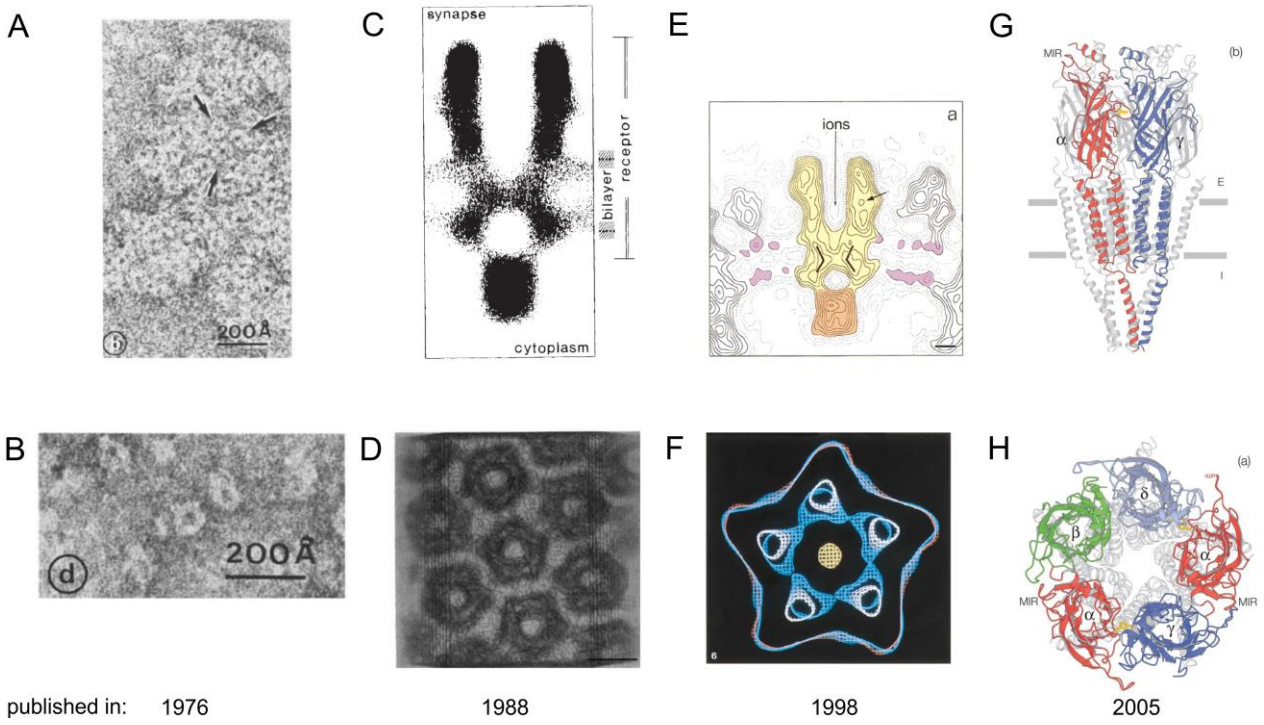

Figure 1 Structure of nACHRs | A) Electron micrographs using 650.000x magnification of nAChRs of *Torpedo* (Cartaud et al., 1973) B) Electron micrographs using 650.000 x magnification nAChRs of *Electrophorus* giving hints for an oligomeric structure including 5 to 6 subunits (Cartaud *et al.*, 1973) C –D) Electron micrograms of tubular vesicles of *Torpedo* at **17Å** resolution in (C) axial section with proposed lipid bilayer positions and (D) section along the tube axis showing the pentameric structure (Toyoshima & Unwin, 1988) E –F) Electron micrograms of tubular vesicles of *Torpedo* at **9Å** resolution in (E) axial section with proposed lipid bilayer positions and (F) section along the tube axis. Opening and closing states could be observed (Unwin, 1998) G-H) Refined structure using crystallographic methods to improve electron micrographs to **4Å** resolution as (G) axial section and (H) section along the tube axis. Different subunits including their secondary structure are depicted.

The nAChR subunits are divided into alpha and beta class subunits depending on the existence of two adjacent cysteines in position 192 and 193 homologous to α1 muscle type receptor. Up to date 9 genes for alpha subunits (α2, α3, α4, α5, α6, α7, α8, α9, α10) and 3 genes for beta subunits (β2, β3, β4) have been cloned from neuronal tissue (CHRA2-10 and CHRNB 2-4). For generating functional receptors

hetero and homopentamers are possible but with subtype restrictions. α-bungarotoxin sensitive receptors can form heteropentamers (α7α8 and α9α10) and homopentamers (α7, α8 and α9). α-bungarotoxin insensitive receptors can only form heteropentamers consisting of α (α2-α6) and β (β2- β4) subunits (Gotti & Clementi, 2004; Gotti *et al.*, 2007). The acetylcholine binding interface is located between an α and a β subunit in heteropentamers, respectively between two α subunits in homopentamers (see Fig. 2). In addition there exist two subunits (α5, β3), which do not take part in ligand binding site formation, which are called accessory subunits (Kuryatov *et al.*, 2008; Gotti *et al.*, 2009).

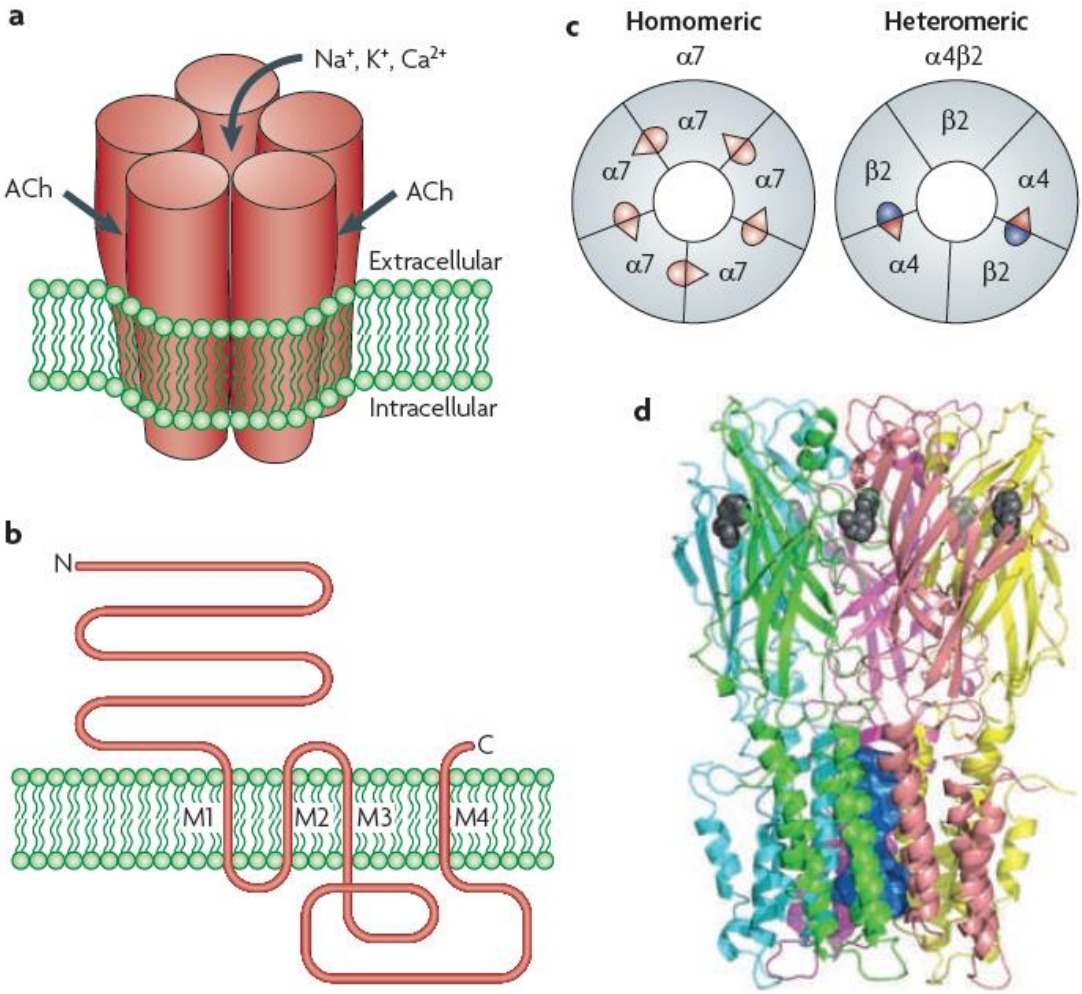

Figure 2 Structure of nAChRs | a) Nicotinic acetylcholine receptors are transmembrane pentameres with variable subunit composition. b) Each subunit consist of a large extracellular N-terminus carrying the Acetylcholine binding site, four transmembran regions as well as an intracellular loop against which the used self-established subtype specific antibodies are directed (David *et al.*, 2010) . c) nAChRs can assemble in homomeric and heteromeric ways. Depicted are the most common nAChR types in the CNS. d) Side view of an alpha 7 homopentamere model showing nicotine molecules in grey and the volume of the ion channel in dark blue (Changeux, 2010)

1.2 Physiological functions:

Nicotinic acetylcholine receptors are responsible for many physiological functions like: maintenance of metabolic tone, arousal, sleep, fatigue, anxiety, central processing of pain, food intake, number of cognitive functions, control of inflammatory processes, neuronal development and degeneration and modulating the release of other neurotransmitters (Cordero-Erausquin *et al.*, 2000; Gotti & Clementi, 2004; Jensen *et al.*, 2005; Albuquerque *et al.*, 2009).

1.3 Pathological issues

Since nAChRs and their perfect distribution and balance have that many physiological functions it is not surprising that they also play a role in numerous diseases like Nicotine addiction, Myasthenia gravis, Autosomal dominant nocturnal frontal lobe epilepsy (ADNFLE), Autism, Attention deficit hyperactivity disorder (ADHD), Depression and anxiety, Alzheimer's disease, Tourette's syndrome and Parkinson's disease (Lindstrom, 1997; Gotti & Clementi, 2004; Jensen *et al.*, 2005; Hurst *et al.*, 2013).

1.4 A spectrum of different nAChR subtypes

Depending on the composition of nAChR subunits, the pharmacological and electrophysiological properties of the nicotinic receptor are altered.

β2 or β4 are needed for a functional hetero oligomeric receptor in neuronal tissue (Champtiaux & Changeux, 2004). Both α and β subunits contribute to the distinct characteristics of subunit composition. β2 containing receptors have 100 times higher affinity for nicotine than β4 containing (Luetje & Patrick, 1991; Picciotto *et al.*, 2000).

The main receptor types of the CNS are α4, β2 and α7 whereas in the periphery α3 and β4 are predominant. (Jensen *et al.*, 2005). α7 homopentamers are typically fast activated, low affinity, high Ca^{2+} permeable receptors and α4β2 are highly affine for acetylcholine and show slow desensitization (Changeux, 2010).

Knockout mice for various nAChR subunits were generated including: α3 (Xu *et al.*, 1999a), α4 (Marubio *et al.*, 1999), α5 (Salas *et al.*, 2003), α6 (Champtiaux *et al.*, 2002), α7 (Orr-Urtreger *et al.*, 1997), α9 (Vetter *et al.*, 1999), β2 (Picciotto *et al.*, 1995), β3 (Cui *et al.*, 2003), β4 (Xu *et al.*, 1999b; Kedmi *et al.*, 2004). None of these created knockout lines show apparent abnormal phenotypes when observed, except α3 inbred knockouts, where 40% of the mice die in the first three days on unknown causes and nearly all remaining animals die in the next 6-8 weeks after weaning (Xu *et al.*, 1999a; Rassadi *et al.*,

2005) reviewed in (Wang *et al.*, 2002). Surprisingly, α3 knockout animals raised as outbred strains live in good health for several months and some females can reproduce (Krishnaswamy & Cooper, 2009).

Although no obvious phenotype is visible on the first glance, mouse nAChR knockout lines show various, more subtle alterations in their autonomic functions and behavior:

β4 knockout mice show minor memory deficits, reduced anxiety, are less prone to nicotine induced antinociception and show decreased nicotine-withdrawal signs (Salas *et al.*, 2004; Salas *et al.*, 2009; Semenova *et al.*, 2012). β2 and α4 knockout mice show less nicotine induced antinociception and reduced nicotine sensitivity. (Marubio et al., 1999). β2 knockouts also show altered avoidance-learning (Picciotto *et al.*, 1995). When both β2 and β4 are knocked out, the mice show impaired growth and are likely to die in the first weeks after birth much like the α3 knockout phenotype described in inbred knockouts (Xu *et al.*, 1999b). α7 knockout animals have impaired vasodilatation when infused with sodium nitroprusside (Franceschini *et al.*, 2000).

1.5 The α5 subunit

The alpha 5 subunit is a special subunit in several ways. First it is, together with β3 with which it shares sequence homology, an accessory subunit which means it must coassemble with another α and β subunit (Boorman *et al.*, 2003). They take not part in orthosteric ligand binding because they are lacking the primary or the complementary components of the Acetylcholine binding site but do influence pharmacology, Ca2+ permeability and desensitization of the nAChR. Therefore the incorporation of α5 allows for changes in pharmacology without the need of changing the receptor number per se (Ramirez-Latorre *et al.*, 1996; Wang *et al.*, 1996; Gerzanich *et al.*, 1998; Gotti *et al.*, 2007).

The α5 subunit is encoded by the CHRNA5 gene, which is clustered on chromosome 15 together with CHRNA3 (α3) and CHRNB4 (β4) with CHRNA5 transcribed in the opposite direction (see Fig. 3) (Eng *et al.*, 1991; Hurst *et al.*, 2013).

Figure 3 The CHRNA5 gene cluster | Transcription of CHRNA5 is in opposite direction than CHRNAB4 and CHRNA3 on their gene cluster. (Hurst *et al.*, 2013)

α5 containing receptors are more sensitive to nicotine and in line with that, the α5 knockout mice show more resistance to nicotine and nicotine induced seizures, especially the α5β4 double knockout.

Generally α5 knockout mice show no obvious phenotype and normal viability (Salas *et al.*, 2003; Jensen *et al.*, 2005; Jackson *et al.*, 2010).

The α5 subunit in particular is highly expressed in the habenula-interpeduncular pathway, the hippocampus and in deeper layers of the cortex and lower expressed in the substantia nigra and in the ventral tegmental area. The cholinergic projections from the median habenula into the IPN called "fasciculus retroflexus" provide a very important connection between the limbic forebrain and the midbrain (Klemm, 2004; Jensen *et al.*, 2005; Leslie *et al.*, 2013).

Our group further identified the superior cervical ganglion (SCG) and interpeduncular nucleus (IPN) as areas of high α5 abundance in the CNS (see Fig. 4).

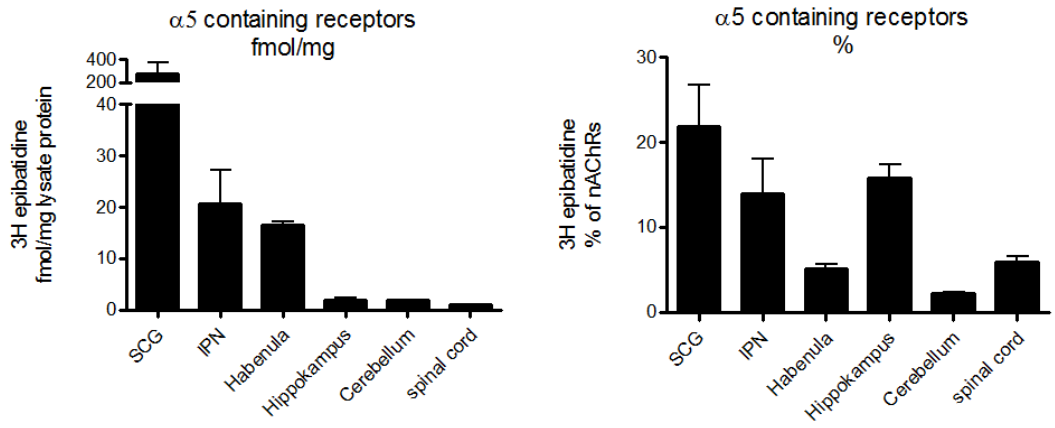

Figure 4 Levels of α5 containing nAChRs in different tissues | data from our lab: (A) Absolute and (B) relative (shown as a percentage of overall hetero-oligomeric receptors precipitated by the combined use of anti-β2 and anti-β4 antibodies) levels of α5-containing receptors in the indicated tissues with SCG and IPN containing the most α5 nAChR - subunits.

1.5.1 Nicotine addiction and smoking behavior

Nicotine addiction and its resulting impacts on human health is one of the most abundant sources for avoidable deaths. Dopaminergic neurons play a big role in behaviors like reward path mechanisms, addiction and stress and the relevant locations are in the dopaminergic midbrain which consists of the substantia nigra and the ventral tegmental area (VTA) projecting to the prefrontal cortex and to limbic and striatal structures like the nucleus accumbens, amygdala, hippocampus and the habenulo-interpeduncular system (Klink *et al.*, 2001; Chinta & Andersen, 2005; Changeux, 2010). Functional magnet resonance imaging studies showed that the most response areas to nicotine injections in subcortical regions were in the ventral tegmental area, substantia nigra, nucleus accumbens and the

thalamus (Suarez *et al.*, 2009). In these regions, especially in the substantia nigra and in the ventral tegmental area, nicotinic acetylcholine receptors are densely expressed and modulate dopamine release in vivo and in vitro. That is eventually a direct mechanism of the implication of nAChRs acting on the dopaminergic system and influencing nicotine addiction (Charpantier *et al.*, 1998; Klink *et al.*, 2001). Additionally nAChRs are modulating glutamatergic and GABAergic neurons in the VTA thereby also influencing the dopaminergic system (Fowler *et al.*, 2008).

Evidence for the implication of the α5 subunit in nicotine addiction gives the observation that α5 knockout mice showed altered nicotine self-administering behavior. When α5 was knocked down with a lentivirus in the median Habenula the mice chose greater nicotine doses for self-administering. After application of a rescue vector, restoring the α5 subunit in the median Habenula, this behavior disappeared and was undistinguishable from wild-type mice. These findings propose a mechanism that the habenulo-interpeduncular pathway including α5 somehow provides an inhibitory motivational signal that controls drug intake. This circuit opposes the positive reward signals provided by the mesoaccumbens (Fowler *et al.*, 2008; Changeux, 2010; Frahm *et al.*, 2011).

Electrophysiological recordings showed decreased firing of α5 knockout VTA neurons in response to nicotine in comparison with wild-type neurons. (Morel *et al.*, 2013)

This established a direct link between mouse studies and human genome wide association studies, as these findings in mouse and rat were in compliance with genome wide association studies in humans. Several groups tested numerous human subjects, including European-American and African-American samples and found a SNP rs16969968 located in the CHRNA5 highly correlating with smoking addiction and lung cancer. This SNP changes an amino acid of CHRNA5 from aspartic acid to asparagine on position 398 (D398N) (Bierut *et al.*, 2008; Hung *et al.*, 2008; Saccone *et al.*, 2009; Morel *et al.*, 2013). Also the amount of α5 expressed influences the risk of nicotine addiction and lung cancer (Wang *et al.*, 2009).

Further hints that the mouse findings apply on the human give the observation that CHRNA 5 sets the amount of nicotine necessary to activate dopaminergic neurons. Morel et al showed that the non-synonymous SNP rs16969968 generates a loss of function of the protein in vivo, resulting in much higher nicotine self-administering doses of tested mice as seen before by other groups.

So the reason that humans carrying that SNP are more prone to nicotine addiction and the resulting health issues, could be that they need more nicotine intake in order to overcome the threshold of the nAChRs modulating their dopaminergic system (Morel *et al.*, 2013).

Notably another SNP was found in the CHRNA5 gene which correlates with lung cancer in patients which never smoked. That concludes that there exists another mechanism of acetylcholine receptors influencing cancer development apart from tobacco use (Wang *et al.*, 2010).

The α5 subunit also seems to play a role in nicotine cessation because α5 knockout mice showed less somatic signs of nicotinic withdrawal symptoms compared to wild –type animals(Jackson *et al.*, 2008).

1.5.2 Attention circuitry

Nicotinic acetylcholine receptors in the medial prefrontal cortex play an important role by modulating acetylcholine release in relation to attentional tasks (Passetti *et al.*, 2000). The α5 subunit in particular is found to be crucial showing reduced nicotinic currents in layer VI pyramidal neurons of α5 knockout mouse brain slices. In living α5 knockout mice the accuracy under high attention demanding tasks was significantly decreased compared to wild-type animals (Bailey *et al.*, 2010).

1.5.3 Pain

Nicotinic acetylcholine receptors have been reported to be involved in the modulation of innocuous and nociceptive pain transmission (Vincler & Eisenach, 2005). In this study, spinal nerve ligation altered gene expression of various genes including the α5 and β2 nicotinic acetylcholine receptors. Expression of these two subunits was significantly increased following post spinal nerve ligation shown by Western blot (Young *et al.*, 2008). α2 and β2 subunits were also found upregulated in the dorsal horn of the spine, 14 days post nerve injury as detected by cDNA microarray (Yang *et al.*, 2004). Vincler showed via immunohistochemical staining the upregulation of α5 in the spine dorsal horn (Vincler & Eisenach, 2004). Knock down of α5 lead to significant decrease of antinociceptive effects of nicotine in mice and was found to maintain mechanic allodynia in rats (Vincler & Eisenach, 2005; Jackson *et al.*, 2010). Additional findings report that the antinociceptive activity of nAChR agonists were diminished in α5 knockout mice as well as they did behave less sensitive to locomotor depression and hyperthermia effects resulting from acute nicotine effect than wild-type animals (Salas *et al.*, 2003; Jackson *et al.*, 2010). These findings strongly suggest that the nicotinic acetylcholine receptor subunit α5 plays a crucial role in pain mechanisms and especially in long term receptor rearrangement. However, recent findings in our lab using α5 knockout mice in several pain models, also using the same experimental settings as Jackson, could not confirm the implication of α5 in neuropathic pain mechanisms but α5 knockout mice showed reduced tolerance to the analgesic effect of nicotine (Xanthos. *et al.*, 2014).

1.6 Antibodies against subunits of nAChRs

Because of the above mentioned involvements of nAChRs in a variety of pathologic diseases there is a great urge for finding specific antibodies. Many different subunits are responsible for different diseases and therefore subunit specific antibodies are needed. Moser *et al* showed that current commercial available antibodies are not useful for most technicques. (Moser *et al.*, 2007) Therefore our group decided to raise antibodies on our own (David *et al.*, 2010; Scholze *et al.*, 2011; Scholze *et al.*, 2012).

1.7 Aim of this study

The aim of this study was to purify polyclonal α5 subunit specific antibodies from newly immunized rabbits and guinea-pigs. To identify whether these newly derived antibodies were capable of binding specifically to its nicotinic acetylcholine receptor subunit antigen, they were subjected to stringent tests including Western Blot, Immunoprecipitation and Immunocytochemistry in native and homologue tissues. Due to the fact that our institute possesses various nAChR subunit knockout mouse lines the specificity can be ultimately tested to provide high quality antibodies contrary to those tested by Moser et al (Moser *et al.*, 2007). A side project consisted of purifying monoclonal anti-α5 antibodies from Hybridoma clones which were generated back in 2002.

Another aim was to identify the subunit composition of the Interpeduncular nucleus (IPN) from P18 mice. For that experiments wild-type, α5-knockout, β2 knockout and β4 knockout mice IPN were immunoprecipitated with α2, α3, α4, α5, β2 and β4 antibodies and analyzed.

2 Material and Methods

2.1 HEK cells cultivation and transfection and harvest

Cultivation

HEK 293 (Human Embryonic Kidney cells 293) cells were kept in culture at 37°C/5% CO_2 in "HEK Complete Medium".

HEK Complete Medium		
Dulbecco's Modified Eagle Medium (DMEM), high glucose+ GlutaMAX	500ml	GIBCO-life technologies
Fetal Calf Serum	50ml	SIGMA
Penicillin-Streptomycin 1000 U/ml	5ml	GIBCO-life technologies
MEM Non-Essential Amino Acids	5ml	GIBC-life technologies

Transfection (4 days)

Day1:

Cells from a 50% grown plate were counted and seeded onto a new plate (Sarstedt Cell+)

	Cells	**HEK Complete Medium**
9.5 cm plate	1.8×10^6	9.0 ml
5.5 cm plate	0.7×10^6	3.5 ml
3.5 cm plate	0.3×10^6	1.5 ml

Day2:

H2O/DNA/CaCl2 was mixed as described in Table 1 and added dropwise to HeBS Buffer(50mM HEPES, 280mM NaCl, 1,5mM Na2HPO4x2H20 pH optimum=7,12 [date:10/12]), while air was bubbled through the buffer. After vortexing and following incubation time of 20minutes the solution was again vortexed and dropped onto the HEK cell plates.

	DNA	**H2O**	**2.5 M CaCl2**	**HeBS**
9.5 cm plate	20 µg DNA	ad 450 µl	50 µl	500 µl
5.5 cm plate	8 µg DNA	ad 180 µl	20 µl	200 µl
3.5 cm plate	3.5 µg DNA	ad 75 µl	8.5 µl	84 µl

Table 1 Pipetting Scheme for HEK Transfections

After 4 hours the medium was exchanged with fresh HEK Complete Medium.

Day4: Harvest

Medium was removed and the plate was washed with 1xPBS (136,9mM NaCl, 2,7mM KCl, 1,8mM KH_2PO_4, 10mM Na_2HPO_4 x $2H_2O$ pH=7,4). Then the cells were scraped off with 2x500µl PBS and transferred into a reaction tube. After centrifugation for 1min at 13000rpm and room temperature the supernatant was discarded and the cell pellet was resuspended in 300µl 2% Triton-X Lysis Buffer (50 mM Tris–HCl pH = 7.5, 150 mM NaCl, 2% Triton X-100, supplemented with one complete mini protease inhibitor cocktail tablet (Roche Molecular Biochemicals, Indianapolis, IN, USA) per 10 mL buffer and stored at -20°C or used subsequently.

2.2 Generation of antibodies

The antibodies used were targeted against the cytoplasmatic loop region between M3 and M4 (see Fig. 6). For the anti-α5 antibody the region between the amino acids (aa) 362-381 (KLLC…EEAE); for anti-β2 between aa 353-422; and for anti-β4 between aa 350-426 were chosen.

These regions were linked with a MBP fusion protein. The Poly-HisTag on the N-terminal end of the fusion protein enables purification via Ni-affinity chromatography. The purified fusion protein is used to immunize rabbits (Mossier *et al.*, 1994; David *et al.*, 2010).

2.3 Immunization of rabbits and guinea pigs

2 rabbits and 4 guinea-pigs were immunized with the previously generated α5 MBP fusion protein (4F3 construct). For the first immunization 100µg α5-MBP fusion protein, 75µl 10xPBS (1369mM NaCl, 27mM KCl, 18mM KH_2PO_4, 100 mM Na_2HPO_4 x $2H_2O$ pH=7,4), 584µl H2O and 1ml Freund Adjuvants (complete) were mixed on ice and emulsified until one droplet of the solution could swim on the surface of cold water without dispersing. The viscous solution was picked up by a syringe and kept on ice until immunization approximately 1 hour later. For the subsequent booster immunizations incomplete Freud adjuvants was used instead of the complete Freud adjuvants. The immunizations were conducted according the immunization scheme below. One of the rabbits S24a died in week 25 of the year 2012 (not shown). Immediately after, another rabbit was freshly immunized and named S24a resulting in a delayed schedule for this animal.

week	animals S23a, S35, S36, S37, S38	S23a bleeding nr	animal S24a	S24a bleeding nr
2012				
15	1. immunization			
19	2. immunization			
23	3. immunization			
	pause			
25		1		
			1.immunization	
26		2		
27		3		
28	bleeding omitted	4		
	4.immunization		2.immunization	
29	pause			
30		5		
31		6		
32		7		
33		8		
	5.immunization		3.immunization	
34	pause			
35		9		1
36		10		2
37		11		3
38		12		4
39		13		5

40	6.immunization / S35, S36, S37, S38 exsanguinated		4.immunization	
41	pause			
42		14		6
43		15		7
44		16		8
45		17		9
46		18		10
47		19		11
48		20		12
49		21		13
50		22		14
51		23		15
52		24		16
2013				
1	bleeding omitted			
2		25		17
3		26		18
4		27		19
5		28		20
6	7.immunization		5.immunization	
7		29		21
8	bleeding omitted			
9		30		22
10		31		23
11		32		24
12		33		25
13		34		26
14		35		27
15	S23a exsanguinated			
16	S24a exsanguinated			

Table 2 Immunization schedule for the rabbits S23a,S24a and the guineapigs S35,S36,S37,S38

As the serum arrived at our department it was incubated for 1hour at 37°C and then stored overnight at 4°C. On the following day it was centrifuged for 15min at 4000rpm and 4°C, the supernatant was transferred into a new tube and again centrifuged for 15min at 4000rpm and 4°C. Again the supernatant was transferred into a new tube and stored at -20°C.

2.4 Generation of affinity columns and coupling of fusion proteins for antibody purification

Expression of GST-α5 fusion protein

4F3 Glycerine culture (Xl1-blue bacteria expressing GST-α5-fusion protein) was plated on LB-Amp plate and incubated over night at 37°C. On the next day a clone of that plate was introduced into 5ml 1xLB-amp medium as an O/D pre-culture and incubated for ~4hours at 37°C and 200rpm.(2xLB rich Medium: 60g Bactotryptophan, 30g Yeast extract, 30g NaCl, H2O ad 2400ml, pH 7,4 after autoclaving addition of 10ml 40% glucose and 2ml 100mg/ml ampicillin). 1,5ml of the O/D preculture were then transferred into 150ml 1xLB-amp medium and incubated over night at 37°C and 200rpm. 3 x 5000ml Erlmayer flasks containing 2L of 1xLB-amp medium each were inoculated with 40ml O/N preculture (1:50) and incubated at 37°C and 180 rpm until OD600 reached 0,5-0,7. Subsequently 1M IPTG was added to induce gene expression. After 2 hours the expression was stopped, the cells were centrifuged for 15minutes at 6000rpm and 4°C, the pellets kept and stored at -20C°. Every pellet was then resuspended in 15ml 6M Guanidin-HCl and stirred for 1hour.

Preparing Ni-NTA Agarose (QIAGEN)

For each column 6ml Ni-NTA Agarose was filled into a 50ml falcon-tube and washed 5x with H2O. The lysed bacteria were centrifuged for 10min at 10000rpm and 4°C (SLA-1500 rotor) and the supernatant was added to the washed Ni-NTA agarose. The mixture was incubated 1,5hours at a swivel table, centrifuged shortly at 400rpm and then transferred to columns. Each column was washed with 1x3ml 6M Guanidin-HCl; 6x 4ml 8M Urea pH=6,3; 1x 1,5M Urea pH=5,8. The protein was eluted with 4x 1,5ml 8M Urea pH=5,9; 6x 2ml 8M Urea pH=4,5.

Quality control of expression and purification

The efficiency of the procedure was controlled by loading the samples which were taken at the most important steps onto a 15% PAGE Gel

Separation Gel 15% Tris/Glycin

3,75ml	dH2O
3,75ml	4xSeparation Gel Buffer (1,5M Tris-HCl, pH=8,8)
7,5ml	30% Acrylamid/Bisacrylamid 29:1
150µl	10% SDS
150µl	10% APS (prepared fresh)
15µl	TEMED

Stacking Gel 5%

2,4ml	dH2O
1,2ml	4xStacking gel buffer (0,5M Tris/HCl pH=6,8)
850µl	30% Acrylamid/Bisacrylamid 29:1
50µl	10% SDS
50µl	10% Ammoniumperoxidisulfae (APS)
5µl	TEMED

First the separation gel was transferred into the casting frame and covered with isopropyl alcohol to allow for a smooth gelatinization edge. After approximately 15min the gel polymerized and was washed with H2O. Excessive H2O removed with tissue, the Stacking gel was added until overflowing and the well-forming comb was added. After polymerization of the Stacking gel the comb was gently removed, the pockets washed with H2O and Running Puffer(25M Tris, 192 mM glycine, 0.1%SDS).

10µl of the column load and flow-through were mixed with 100µl H20, 200µl Methanol, 100µl Chloroform, vortexed and centrifuged for 5min at 13000rpm and room temperature. The upper phase was discarded and to the clear lower and milky interphase 400µl Methanol was pipetted. After another vortex step, the solution was centrifuged for 10min at 13000rpm and room temperature, the supernatant discarded, the pellet was dried and 15µl 1xSample Buffer was added. The pellets from induced / non-induced samples were also mixed with 15µl 1xSample Buffer 10µl eluate samples were mixed with 4µl 4xSample Buffer (250mM Tris-HCl pH=6,8, 20% 2-Mercaptoethanol, 8% SDS, 0,04% Pyranin Y) and 2µl H2O. Samples were denatured for 15mins at 65°C and centrifuged for 1min at 13200rpm, except the marker (SeeBlue Plus 2, Invitrogen) and loaded onto the gel. The proteins were separated at 200V, 200mA (CONSORT E831 power supply) for app. 1 hour in Running Puffer (25M Tris, 192 mM glycine, 0.1%SDS).

Subsequently the gels were washed with 3x dH2O 5min, then stained for 1hour with Simply Blue Safe Stain (Invitrogen) and then destained by washing 3x with dH2O.

Concentration of the GST-α5 fusion protein

The eluates with the highest protein content (as judged by the size of the acrylamide gel band) were measured using the Pierce BCA (bicinchoninic acid) Protein Assay Kit (Thermo Scientific) according to the manufacturer's manual, pooled and diluted 1:1,6 with 1xQE (5xQE: 22,25g Na2HPO4*2H2O, 43,8g NaCl, H2O ad 500ml, pH=8,0) to reduce urea concentration which would also bind to the amino-binding sites of the later used affi-gel but is at the same time necessary for keeping the protein in solution. The pH was brought to the iso-electric point of the protein to remove its charge (pH=6,6) with NaH2PO4.

The GST-α5 fusion protein was then concentrated using a prewashed Centricon with molecular weight cut off: 10 000. α5 fusion protein solution was stepwise loaded and centrifuged for 5min at 4000rpm. The flow-through was discarded and α5-fusion protein was again added on top of the centricon column. After every centrifugation step the concentrated solution was pipetted up and down to prevent clogging and precipitation of the protein.

Coupling of the fusion protein onto the column

The concentrated protein was centrifuged again (5min, 4000rpm) and added to a 15ml falcon tube filled with 6ml pre-washed Affi-Gel 10 (Biorad). After an incubation time of 1,5h on a rolling device at 4°C 1M Ethanolamin pH=8,0 was added and incubated for 1h to saturate remaining free binding sites of the gel.

The column material was transferred into prewashed columns, waited for it to settle and then washed with

30ml 1xPBS (136,9mM NaCl, 2,7mM KCl, 1,8mM KH_2PO_4, 10mM Na_2HPO_4 x $2H_2O$ pH=7,4)
15ml Glycin-Elution Buffer (150mM NaCl , 100mM Glycine pH=2,45)
10ml 1xPBS
30ml basic elution buffer (150mM NaCl, 100mM Na2HPO4*2H2O)
20ml 1xPBS
30ml acidic elution buffer (150mM NaCl, 100mM NaH_2PO4 x H_2O, pH=2,45)
20ml 1xPBS

The columns were stored with 5ml 1mM NaN3 on top of the column to prevent microbial growth.

2.5 Antibody purification

Preparations

The affinity columns stored at 4°C and the blood sera stored at -20°C were brought to room temperature (app. 30minutes). After thawing of the blood sera 1/9 of the volume was added as 10xPBS. In the meantime Eppendorf tubes were filled with 100µl Neutralisation Buffer (1M NaH_2PO_4 x H_2O). The columns were washed with 20ml 1xPBS (136,9mM NaCl, 2,7mM KCl, 1,8mM KH_2PO_4, 10mM Na_2HPO_4 x $2H_2O$ pH=7,4)

Application of Serum

A blue syringe needle was attached to the column (Ø=0,6mm) to reduce flow-rate and the serum was applied through moistened folded filter.

Elution

The flow-through was collected in a 50ml vial for a second purification run and the column was washed with 50ml 1xPBS. For the elution 1ml Basic Elution Buffer (150mM NaCl, 100mM Na_2HPO_4 x $2H_2O$, pH=11,5) was applied with a pipette and the eluate was collected in 1,5ml Eppendorf tubes containing 100µl Neutralisation Buffer. The tubes were immediately shaken and stored at 4°C.

Washing

After use the column was washed in the following order with:

- 20ml Basic Elution Buffer (150mM NaCl, 100mM Na_2HPO_4 x $2H_2O$, pH=11,5)
- 20ml 1xPBS (1,369mM NaCl, 27mM KCl, 18mM KH_2PO_4, 100mM Na_2HPO_4 x $2H_2O$ pH=7,4)
- 20ml Acidic Elution Buffer (150mM NaCl, 100mM NaH_2PO4 x H_2O, pH=2,45)
- 30ml 1xPBS (1,369mM NaCl, 27mM KCl, 18mM KH_2PO_4, 100mM Na_2HPO_4 x $2H_2O$ pH=7,4)

To prevent microbiological contamination1xPBS containing 0,1%Sodium azide was added on top of the column.

Protein concentration determination

The Eluates were screened using a Bradford Assay. To 5 parts Bradford stock reagent (100mg Coomassie Blue-G250, 50ml Methanol, 100ml 85% phosphoric acid, add H20 to 1000ml) 4,5 parts dH2O were added to obtain the ready to use solution (5+4,5). On a 96 well plate 5µl of Eluate were mixed with 100µl

Bradford solution. After photometric detection at 595nm the eluates with an OD of more than 0,05 were pooled and the protein content analyzed precisely with Pierce BCA (bicinchoninic acid) Protein Assay Kit (Thermo Scientific) according to the manufacturer's manual. Hereby 10µl of pooled eluate was mixed with 200µl freshly mixed Pierce- BCA reagent (50 parts solution A + 1 part solution B) on a 96-well plate. After 30minutes incubation at 37°C samples were analyzed at 562nm.

2.6 Immunoprecipitation

Dissected tissue (IPN (Interpeduncular Nucleus) and SCG (Super Cervical Ganglion from 18days old wt and α5-KO mice) stored at -80°C was resuspended in 2% Triton-X Lysis Buffer (50 mM Tris–HCl pH = 7.5, 150 mM NaCl, 2% Triton X-100, supplemented with one complete mini protease inhibitor cocktail tablet (Roche Molecular Biochemicals, Indianapolis, IN, USA) per 10 mL buffer. After one 5sec ultrasonic pulse at 40% power (Bandelin Sonoplus UW 2200) the homogenized tissue was incubated for 2h at 4°C on ice without shaking. Pure lysate of the tissue was obtained by centrifugation of the homogenized tissue for 15min, 13000rpm at 4°C and discarding the pellet. 130 µl Lysate was incubated with 20µl 10nM [3H]Epibatidine and 5µg antibody on a shaking platform over night at 4°C. Unspecific binding was evaluated by adding 300µM Nicotine (0,6µl) to half of the samples.
Heat-killed formalin-fixed Staphylococcus aureus cells, expressing protein A on their membrane (Standardized Pansorbin cell; Calbiochem, San Diego,CA,USA) were centrifuged at 5000 rpm for 5 minutes at 4°C. Pansorbin-pellets were washed twice with IP-High (50mMTris-HCl pH=8.3, 600mM NaCl, 1 mM EDTA, 0.5% TritonX-100), once in IP-Low (50 mM Tris-HCl pH=8.0, 150 mM NaCl, 1 mM EDTA, 0.2% Triton X-100), and resuspended with IP-Low.

20µl of this prewashed Pansorbin cells was added to the Lysate Mix (including solubilized receptor, epibatidine and antibody) and incubated on the shaking platform at 4°C for 2 hours.
Afterwards the samples were centrifuged for 5minutes, 5000rpm at 4°C and washed twice with IP-High and once with IP low while taking care that the pellet was not disturbed.

Finally the pellets were resuspended in 200µl 1N NaOH, transferred into 5ml Sarstaedt vials, prefilled with 2ml Scintillation cocktail (Rotaszint Eco Plus, ROTH), and subjected to liquid scintillation counting (Packard TRI-CARB 2100TR)

2.7 Immunocytochemistry of SCG and HEK cells

For immunocytochemistry SCGs of 3 to 6 day old (P3 - P6) wildtype and α5-KO mice were dissected and cultured on glass slides by Karin Schwarz. 10 000 cells were placed into 8mm glass rings on laminin-coated glass slides in 3,5cm cell plates. The cells were incubated at 37°C / 5% CO2 for 3 to 6 days prior use (DIV 3 – DIV6).

HEK 293 cells were transfected as described in 2.1 but for immunocytochemistry the cells were seeded on 3,5cm plates, with three laminin-coated glass slides placed on the bottom and instead of harvesting the cells were fixed.

The culture medium was removed and the plates were washed 3x with PBS. Subsequently 2-3ml cold 4% PFA was added (1g PFA, 15ml H2O, 2 drops NaOH to dissolve the PFA at 60°C, +2,5ml 10xPBS, pH=7,35, H2O ad 25ml – prepared fresh for one week) and incubated for 10 minutes at room temperature. PFA was removed and 2-3ml glycine in PBS (110mg Glycine in 15ml 1xPBS) was added for 10 minutes at room temperature. To block unspecific binding the plates were covered with blocking solution containing 3%NDS (Normal Donkey Serum) in 0,2% Triton / PBS (450µl NDS, 30µl Triton X-100 in 15ml 1xPBS) for 30 minutes at room temperature. Then primary antibody diluted in blocking solution was incubated for 1 hour followed by 3 x 5min washing steps with 0,2%Triton/PBS. Afterwards the secondary antibody diluted in blocking solution was applied for 1hour in the dark. Subsequently the plates were washed 3x5min washing steps with 2-3ml 0,2% Triton/PBS, shortly immersed in H2O and embedded with Prolong Gold Anti Fade Reagent (Invitrogen).

primary antibodies	**concentration [ng/µl]**	**dilution for 0.4µg/ml**
α5 S35 guineapig polyclonal	61	1:152.5
α5 S36 guineapig polyclonal	59	1:147.5
α5 S37 guineapig polyclonal	43	1:107.5
α5 S38 guineapig polyclonal	86	1:215
α5S23 pool rabbit polyclonal	605	1:1500
α5 S23a minipool rabbit polyclonal	320	1:800
α5 S23a/3 rabbit polyclonal	688	1:1700
α5 S23a/9 rabbit polyclonal	345	1:860
α5 S23a/10 rabbit polyclonal	321	1:800
α5 S23a/15 rabbit polyclonal	379	1:950
α5 S23a/16 rabbit polyclonal	277	1:692

a5 S24a minipool rabbit polyclonal	187	1:460
α5 S24a/1 rabbit polyclonal	228	1:570
α5 S24a/7 rabbit polyclonal	263	1:660
α5 S24a/15 rabbit polyclonal	221	1:552
α4 S26 rabbit polyclonal	410	1:1000
β4 S05 rabbit polyclonal	139	1:347.5
		working dilution
Actin Chemicon MAB1501 mouse monoclonal		1:1000
Antiflag BioM2 Sigma (1µg/µl Aliquots) mouse monoclonal		1:100
MAP2 (Cat#AB5622, Lot:#1966895)rabbit-Monoclonal		1:1000
secondary antibodies		**working dilution**
Alexa rabbit 488		1:1000
Alexa mouse 568		1:1000
Alexa goat anti guinea pig 647		1:200

Table 3 Immunocytochemistry antibody dilutions

2.8 Cryosections for immunocytochemistry

Preparation of tissue for cryo sectioning

Mice were anaesthetized with CO2 and sacrificed by cervical dislocation. The heart was laid open, a hollow needle was inserted into the left ventricle of the heart and the right atrium was opened. After the first perfusion with 1xPBS for 5 minutes using a peristaltic pump, the liver turned white, indicating proper flow through the whole body circulation system. Then the animal was perfused for 10 minutes with 4%PFA. Subsequently the animal was decapitated, the brain was dissected and further fixed with 4%PFA for 7hours. The brains were then washed with 2x 5min with 1xPBS. Next the brains were immersed in 1xPBS with 10% Sucrose (pH=7,4) until the brain sinks to the bottom of the tube (app. 30 min) and then immersed in 1xPBS with 30% sucrose (pH=7,4) over night. The brains were frozen in -40°C cold Isopentan and either immediately used for slicing or stored at -80°C.

Cryosection of mouse brains

The frozen brains were rapidly taken to the precooled cryotome without thawing the tissue. The tissue was initially cut with a razor knife on the dorsal side, removing the hippocampus, in order to allow attachment into the cryotome. The cut brain was attached with Tissue-Tek O.C.T. compound onto the specimen holder. Using Stereotaxic Atlas of the Rat Brain – 1967 edition for orientation, 25µm slices towards the regions of interest, medial Habenula (Interaural 4890µm Fig32.b.) and IPN (Interaural

2189µm), were cut in 15µm slices. These slices were picked up on SFPC Superfrost Plus white, adhesive, 90°cut, CELLO specimen sides avoiding water condensation. The slides were then immediately used for immunocytochemistry or stored at -20°C.

2.9 Immunocytochemistry of Kryoslides

The prepared specimen slides were thawed and dried for a minimum of 15minutes. The tissue slices were encircled with a Fat-pen (Dako) and dried. The slices were washed 3x with 1xPBS and then permeabilized with 0,2%Triton/PBS for 20minutes.

To block unspecific binding the plates were covered with blocking solution containing 3%NDS (Normal Donkey Serum) in 0,2% Triton / PBS (450µl NDS, 30µl Triton X-100 in 15ml 1xPBS) for 90minutes at room temperature. Then primary antibody diluted in blocking solution was incubated for 1 hour followed by 3 x 5min washing steps with 0,2%Triton/PBS. Afterwards the secondary antibody diluted in blocking solution was applied for 1hour in the dark. Subsequently the plates were washed 3x5min washing steps with 2-3ml 0,2% Triton/PBS, shortly immersed in H2O and embedded with Prolong Gold Anti Fade Reagent (Invitrogen). Antibody dilutions were prepared as described in section 2.8

2.10 Western Blot

Separation Gels were casted according the following recipe:

Separation Gel 10% Tris/Glycin

6ml	dH2O
3,75ml	4xSeparation Gel Buffer (1,5M Tris-HCl, pH=8,8)
4,95ml	30% Acrylamid/Bisacrylamid 29:1
150µl	10% SDS
150µl	10% Ammoniumperoxidisulfat (APS) (prepared fresh)
15µl	TEMED

Stacking Gel 5%

2,8ml	dH2O
1,2ml	4xStacking gel buffer (0,5M Tris/HCl pH=6,8)

850µl	30% Acrylamid/Bisacrylamid 29:1
50µl	10% SDS
50µl	10% Ammoniumperoxidisulfat (APS)
5µl	TEMED

100µg tissue samples were resuspended in 4xSamplebuffer (250mM Tris-HCl pH=6,8, 20% 2-Mercaptoethanol, 8% SDS, 0,04% Pyronin Y). Samples were denatured for 15mins at 65°C and centrifuged for 1min at 13200rpm, except for the marker. Proteins were separated at 200V, 200mA (CONSORT E831 power supply) for app. 1 hour.

After SDS Electrophoresis gels are blotted onto a PVDF membrane (Immobilon-P, Millipore IPVH0010) using the "Tank-Blotting" Technique. The pre-wetted membranes and gels are immerged in Transfer Buffer (25 mM Tris, 19 mM glycine, 0.01%SDS, 20% Methanol). Proteins were blotted for 2h at 25V and 200mA (CONSORT E831 power supply). The efficiency of line separation and blotting was judged with Ponceau-Staining. Therefore the blot was covered with Panceau S Solution (10xPanceau S: 2%Panceau S, 30% trichloroacetic acid, 30% sulfosalicylic acid) until bands were visible. For partial destaining, to mark the corresponding lanes with a pencil, H2O was used. After total destaining with 1xPBS the marked strips were excised. To prevent unspecific binding of the antibodies the PVDF membrane strips were incubated in Blockingbuffer (5% non-fat dry milk powder in PBS, 0,1% Tween 20) for 1h followed by incubation with primary antibody diluted in Blockingbuffer (final concentration 1µg/ml) over night at 4°C. After another washing step for 3x15mins with Washingbuffer (1,5% non-fat dry milk powder in PBS, 0,1% Tween20), the secondary antibody diluted 1:10000 in Washingbuffer was incubated for 1h at room temperature. Blots were visualized with the Millipore Immobilon Western HRP Chemiluminescence Kit and photographs were taken with Biorad ChemidocImag.

3 Results

When a rabbit or a guinea-pig was immunized it was named “S” with a number added to the end. Its blood was collected on a weekly basis and numbered consecutively. In this work 35 blood samples of the rabbit S23a and 27 blood samples of rabbit S24a were collected and purified using affinity chromatography columns. “Minipools” of S23a and S24a were created by pooling a small aliquot of the first 20 blood samples. The blood samples of the four guinea-pigs S35, S36, S37 and S38 were not taken on a weekly basis but the animals were exsanguinated 35 weeks after the initial immunization (see Table 2).

To analyze if the purified antibodies bind specifically and quantitatively to the corresponding subunit, a variety of tests with wild-type and knock-out mouse tissue as well as transfected HEK-293 cells were conducted. The method of choice is immunoprecipitation as it is well established in our laboratory and grants sufficient limit of detection. Furthermore we tried whether the new purified anti-α5 antibodies from rabbit or guinea-pig was able to stain their antigen in immunohistochemical methods.

Finally the nAChR subunit composition of the mouse IPN was investigated using various subunit specific antibodies in immunoprecipitation.

3.1 Antibody purification

3.1.1 Rabbits S23a, S24a

Blood samples of the rabbits were taken weekly and were further purified using affinity columns. Fig. 5 shows the gained amount of antibody per blood sample. The graph shows 20 blood samples which are used to generate the minipools. The correlation between boost-immunization and higher antibody yield is sometimes seen but clearly visible is the initial decrease of antibody concentration after the first immunization.

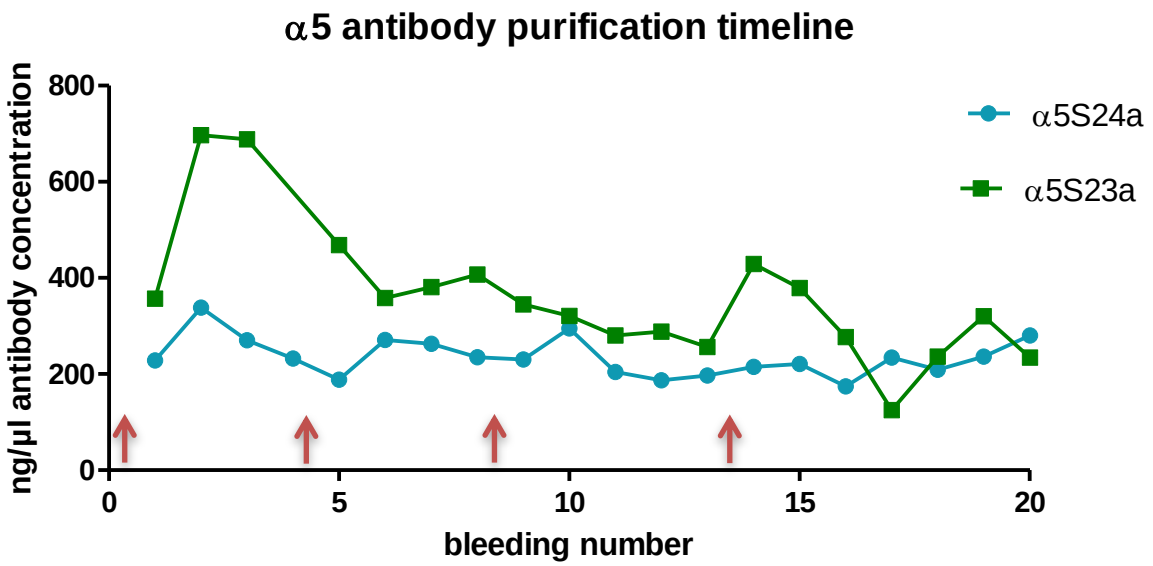

Figure 5 antibody purification timeline | Two rabbits were immunized to generate anti-α5 antibodies. Antibodies were purified using affinity columns. The antibody concentrations are plotted against the time point of bleeding. The red arrows indicate timepoints of boosting immunizations.

These purified antibodies from 20 blood samples were then pooled as seen in Table 4 and Table 5. This resulted in two antibody pools, which resembled the average with neglecting fluctuations in the quality of the antibodies. The calculated estimate of the S23a pool concentration was 360ng/µl, the measured concentration was 320ng/µl. The calculated estimate of the S24a pool concentration was 230ng/µl and the measured 187ng/µl.

	bleeding	aliquot no.	ml	mg/ml	mg		for 1 ml Pool:		fo 50 ml Pool	
α5 S23a	1	6	9.9	**0.357**	3.53		96.59	µl	4.83	ml
α5 S23a	2	4	6.6	**0.697**	4.60		64.39	µl	3.22	ml
α5 S23a	3	2	3.3	**0.688**	2.27		32.20	µl	1.61	ml
α5 S23a	4				0.00		0.00	µl	0.00	ml
α5 S23a	5	3	5.5	**0.468**	2.57		53.66	µl	2.68	ml
α5 S23a	6	3	4.4	**0.358**	1.58		42.93	µl	2.15	ml
α5 S23a	7	3	5.5	**0.381**	2.10		53.66	µl	2.68	ml
α5 S23a	8	3	4.4	**0.407**	1.79		42.93	µl	2.15	ml
α5 S23a	9	3	4.4	**0.345**	1.52		42.93	µl	2.15	ml
α5 S23a	10	3	5.5	**0.321**	1.77		53.66	µl	2.68	ml
α5 S23a	11	3	5.5	**0.28**	1.54		53.66	µl	2.68	ml
α5 S23a	12	4	6.6	**0.288**	1.90		64.39	µl	3.22	ml
α5 S23a	13	2	2.2	**0.256**	0.56		21.46	µl	1.07	ml
α5 S23a	14	2	3.5	**0.429**	1.50		34.15	µl	1.71	ml
α5 S23a	15	6	9.9	**0.379**	3.75		96.59	µl	4.83	ml
α5 S23a	16	5	8.8	**0.277**	2.44		85.85	µl	4.29	ml
α5 S23a	17	5	7.7	**0.125**	0.96		75.12	µl	3.76	ml
α5 S23a	18	2	2.2	**0.236**	0.52		21.46	µl	1.07	ml
α5 S23a	19	2	2.2	**0.320**	0.70		21.46	µl	1.07	ml
α5 S23a	20	3	4.4	**0.234**	1.03		42.93	µl	2.15	ml
sum:			**102.50**	**ml**	**36.63**	**mg**	**1000.00**	**µl**	**50.00**	

Table 4 α5 S23a Minipool | The purified antibodies of 20 bloodsamples were pooled to overcome antibody quality fluctuations, which occur in a biological system over time.

	bleedins	aliquot no.	ml	mg/ml	mg		for 1 ml Pool:		for 50 ml Pool	
α5 S24a	1	5	7.7	**0.228**	1.76		69.68	µl	3.48	ml
α5 S24a	2	2	3.3	**0.338**	1.12		29.86	µl	1.49	ml
α5 S24a	3	2	2.2	**0.27**	0.59		19.91	µl	1.00	ml
α5 S24a	4	2	2.5	**0.232**	0.58		22.62	µl	1.13	ml
α5 S24a	5	5	7.7	**0.188**	1.45		69.68	µl	3.48	ml
α5 S24a	6	2	2.2	**0.271**	0.60		19.91	µl	1.00	ml
α5 S24a	7	3	4.4	**0.263**	1.16		39.82	µl	1.99	ml
α5 S24a	8	5	8.4	**0.235**	1.97		76.02	µl	3.80	ml
α5 S24a	9	4	6.6	**0.23**	1.52		59.73	µl	2.99	ml
α5 S24a	10	2	3.3	**0.295**	0.97		29.86	µl	1.49	ml
α5 S24a	11	6	9.9	**0.204**	2.02		89.59	µl	4.48	ml
α5 S24a	12	5	7.7	**0.187**	1.44		69.68	µl	3.48	ml
α5 S24a	13	3	5.5	**0.197**	1.08		49.77	µl	2.49	ml
α5 S24a	14	3	5	**0.215**	1.08		45.25	µl	2.26	ml
α5 S24a	15	3	5.5	**0.221**	1.22		49.77	µl	2.49	ml
α5 S24a	16	4	6.6	**0.174**	1.15		59.73	µl	2.99	ml
α5 S24a	17	4	6.6	**0.234**	1.54		59.73	µl	2.99	ml
α5 S24a	18	4	6.6	**0.209**	1.38		59.73	µl	2.99	ml
α5 S24a	19	3	4.4	**0.236**	1.04		39.82	µl	1.99	ml
α5 S24a	20	3	4.4	**0.280**	1.23		39.82	µl	1.99	ml
sum:			**110.50**	**ml**	**24.89**	**mg**	**1000.00**	**µl**	**50.00**	

Table 5 α5 S24a Minipool | The purified antibodies of 20 bloodsamples were pooled to overcome antibody quality fluctuations, which occur in a biological system over time.

3.1.2 Guineapigs S35, 36, S37, S38

The guinea-pig blood was retrieved in a single exsanguination rather than a weekly blood withdrawal. The obtained antibody concentrations after affinity column purifications are listed below.

antibody	concentration	amount
α5 S35 guineapig polyclonal	61 ng/µl	3.3 ml
α5 S36 guineapig polyclonal	59 ng/µl	2.2 ml
α5 S37 guineapig polyclonal	43 ng/µl	3.3 ml
α5 S38 guineapig polyclonal	86 ng/µl	2.2 ml

3.2 Antibody characterization using IP

3.2.1 Rabbit antibodies α5S23a and α5S24a on heterologous tissue

Rabbit antibodies were first tested on non-native tissue. Therefore HEK-293 cells were transfected with plasmids carrying the respective nAChR subunit (Putz *et al.*, 2008). Heterologous environment like HEK-293 cells *or xenopus laevis* oocytes are able to express functional receptors given the respective subunits (Cooper *et al.*, 1991; Nelson *et al.*, 2001).

This test in a heterologous system is the first step to see whether the antibody binds to its antigen and needs further testing because the expression is much higher than in native tissue. The HEK cells expressing α4 or β2 act as a negative control as they do not express the α5 subunit but ensure general transfection. The efficacy of the anti-α5 antibody, which was generated by immunizing rabbits with the loop region of the α5-subunit, was probed on receptors generated by replacing the cytoplasmic loop of the β2 subunit by the loop of α5, and by co-expression of this chimera with α4 in HEK-293 cells (see Fig. 6).

Transfection efficiency was about 10-20 %. The new tested antibodies α5S23a and α5s24a show the same specificity and efficacy as the old and well characterized α5S23 (David *et al.*, 2010). For the transfected HEK-293 cells with the α5 loop the α5 antibodies precipitated 100% of the receptors, and in the negative control they precipitated 0%(see Fig. 7).

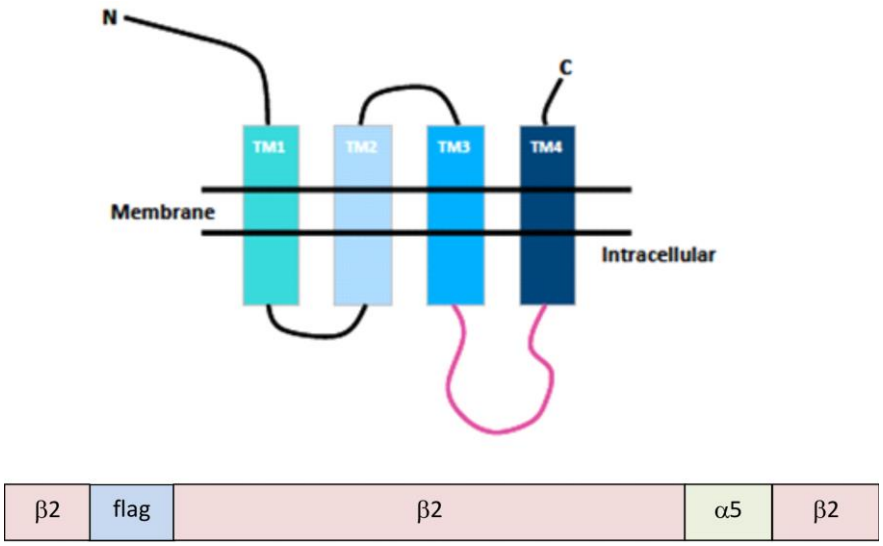

Figure 6 scheme of the nAChR Chimera | structural overview of the nAChR construct with the inserted α5 region highlighted in pink. On the lower panel the signalpeptid – flag – β2 – N-terminus transmembrane domain 1-3 – α5 Loop – β2 transmembrane domain 4 and C-terminus are shown schematically.

Fig 6 shows a schematic representation of the chimeric nAChR construct used to test the efficacy of the anti-α5 antibody. Most of the sequence corresponds to the β2 subunit, only the loop region (shown in red) is replaced by the homologous sequence of the α5-subunit. At the N-terminal end a FLAG-amino acid sequence (DYKDDDDK) followed by a linker region (AGS)6x was introduced immediately after the sequence of the signal peptide in order to enable the detection with an anti-FLAG antibody.

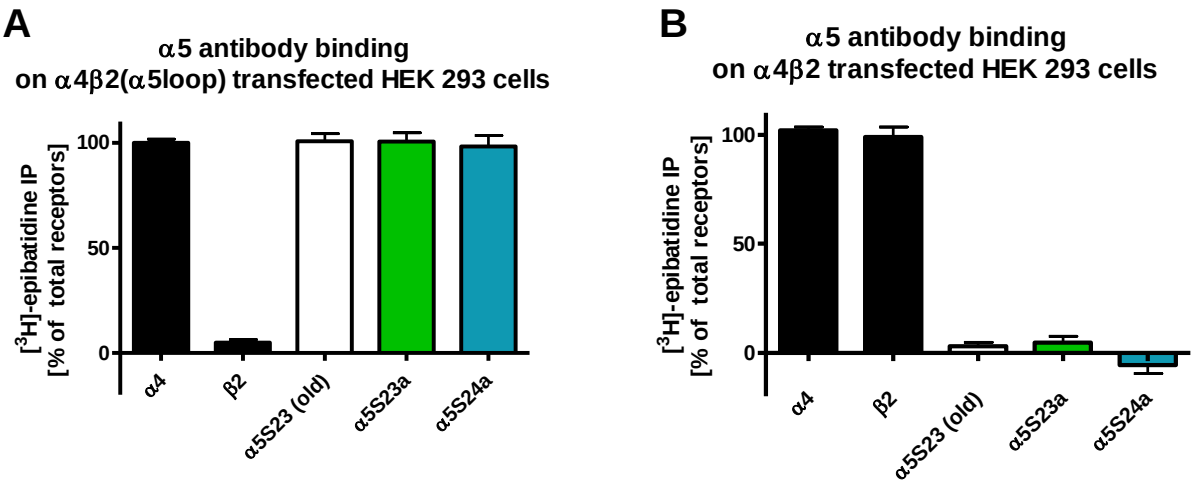

Figure 7 Levels of α5 as detected by the new rabbit S23a and S24a anti-α5 antibodies on transfected HEK-293 cells | solubilized (A) α4β2 transfected HEK cells with the β subunit containing the α5 intracellular loop and (B) α4β2 transfected HEK cells acting as a negative control were labeled with 1nM [^{3}H] Epibatidine and immunoprecipitated using S23a and S24a anti-α5 antibodies. The result is shown as the percentage of total receptors. The amount of receptors precipitated with anti-α4-antibodies is considered 100% . The data shows mean ±SEM of two experiments whereas every datapoint was measured in duplicates.

3.2.2 Rabbit antibodies α5S23a and α5S24a on native tissue

To confirm the results provided by experiments on heterologous tissue, native tissue was further on used to specify the new anti-α5 antibodies in comparison to the old α5s23. The Superior Cervical Ganglion (SCG) contains homopentamers consisting of α7 subunits and heteropentamers containing α3, α4, α5, β2 and β4. (David *et al.*, 2010) This region was chosen as it contains high amounts of α5 (see Fig. 4) and was therefore also used to characterize the former α5S23 antibody. The newly obtained antibodies did not precipitate the same number of receptors as α5s23. α5S23a precipitated only about 30% of the existing α523 antibody (see Fig. 8).

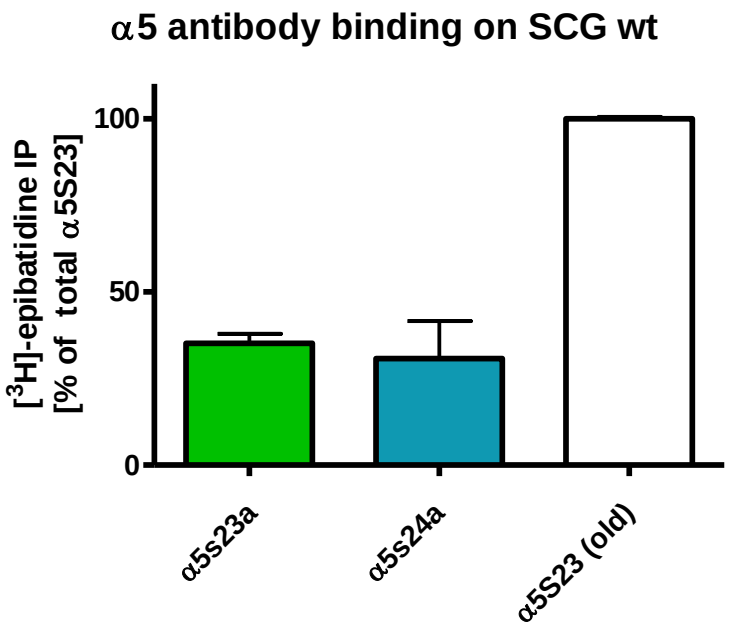

Figure 8 Levels of α5 as detected by the new rabbit S23a and S24a anti-α5 antibodies on wild-type SCG | solubilized SCG from P18 wild type mice were labeled with 1nM [^{3}H] Epibatidine and immunoprecipitated using S23a and S24a anti-α5 antibodies. The results are shown as the percentage of the well characterized previous S23 anti-α5 antibody. The data shows mean ±SEM of three experiments whereas every datapoint was measured in duplicates.

As the Interpeduncular nucleus (IPN) has the second highest amount of α5 nAChR subunits it was also used in the present study. In wild type IPN tissue α5S23 precipitated 24,8 ± 3,7 fmol/mg lysate protein, the new purified antibodies α5S23a 11,3 ± 1,0 fmol/mg lysate protein and α5S24a 11,3 ± 0,6 fmol/mg lysate protein. α5S23 precipitated 6,7 ± 0,7 % of total receptors, the new purified antibodies α5S23a 3,1 ± 0,1 % and α5S24a 3,1 ± 0,2 % of total receptors (see Fig.9 Panels A & B). In α5 knockout IPN α5S23 precipitated 2,3 ± 1,5 fmol/mg lysate protein, the new purified antibodies α5S23a 0,9 ± 0,2 fmol/mg lysate protein and α5S24a 0,8 ± 0,4 fmol/mg lysate protein. α5S23 precipitated 0,6 ± 0,4 % of total

receptors, the new purified antibodies α5S23a 0,4 ± 0,2 % and α5S24a 0,3 ± 0,1 % of total receptors (see Fig.9 Panels C & D).The overall number of [^{3}H]-epibatidine binding sites was determined by combined precipitations with anti-β2 plus anti-β4 antibodies.

In contrast to HEK cells, where all three anti-α5-antibodies precipitated equal amounts, in the IPN only about half as many receptors were precipitated by the new antibodies compared to the well-established a5S23 (see Figure 9 A+B). All of the tested antibodies proved to be highly specific, as they did not precipitate any receptors from the IPN of KO mice.

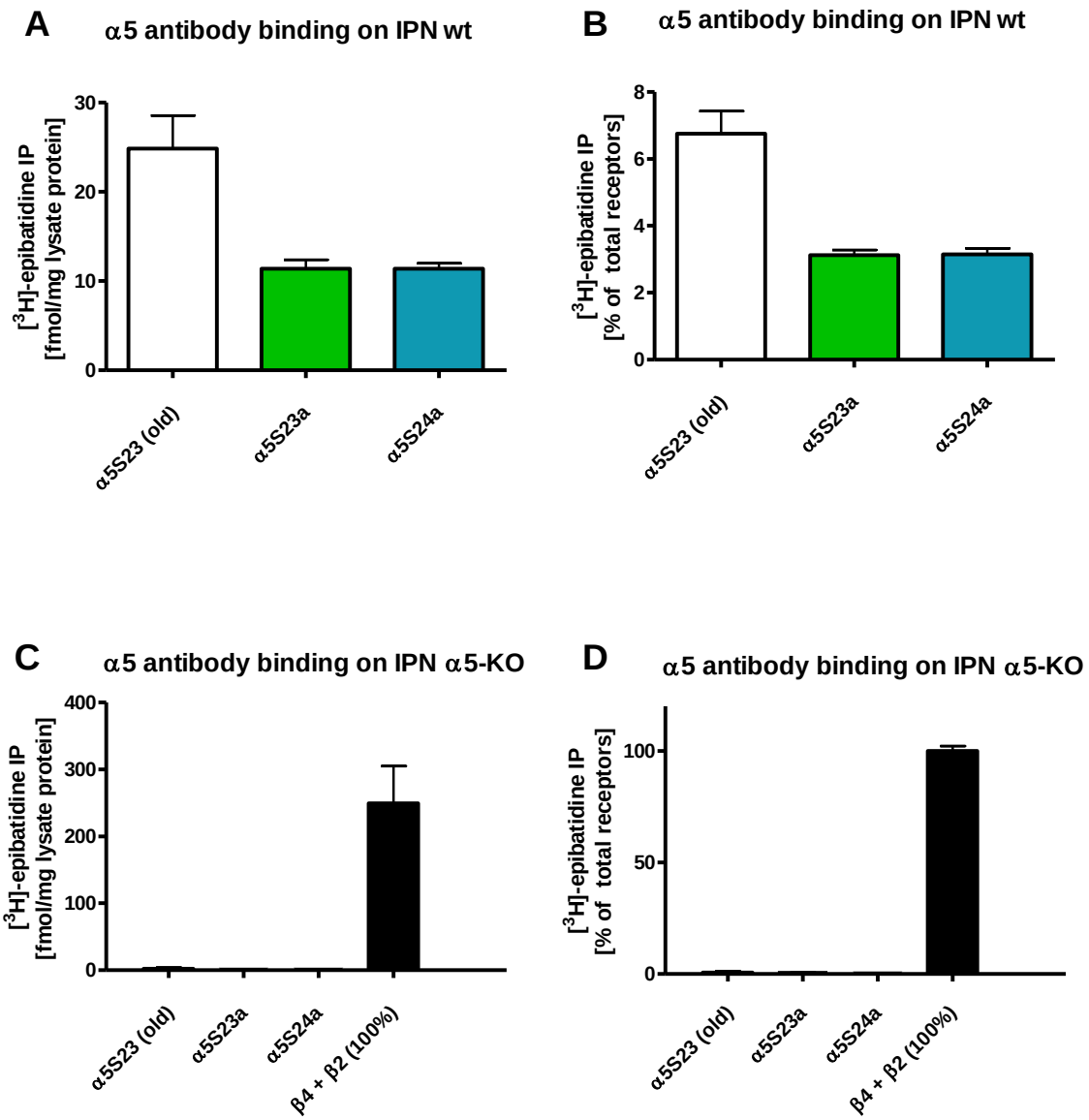

Figure 9 Levels of α5 as detected by the new rabbit S23a and S24a anti-α5 antibodies on wild-type and α5 knockout IPN | (A) and (B) solubilized IPN from P18 wild type mice were labeled with 1nM [^{3}H] Epibatidine and immunoprecipitated using S23a and S24a anti-α5 antibodies. The results are shown (A) as the absolute amount of precipitated nAChR subunit in fmol/mg lysate protein and (B) as the relative amount of nAChR in respect to the total amount of receptors (total receptors was determined by combined precipitations with anti-β2 plus anti-β4 antibodies). (C) and (D) solubilized IPN from P18 α5-knockout mice were labeled with 1nM [^{3}H] Epibatidine and immunoprecipitated using S23a and S24a anti-α5 antibodies. The results are shown in (C) as the absolute amount of precipitated nAChR subunit in fmol/mg lysate protein and (D) as the relative amount of nAChR in respect to the total amount of receptors. The data shows mean ±SEM of four experiments whereas every datapoint was measured in duplicates.

3.3 Antibody characterization using immuncytochemistry

The new antibodies were also tested for their quality in immunocytochemical stainings of heterologous and native cells and in immunohistochemical stainings of brain slices.

3.3.1 On transfected HEK_293 cells Rabbit antibodies α5S23a and α5S24a recognize a5-containing receptors specifically

HEK-293 cells were transfected with α4 and β2(α5), a β2 subunit where the loop region was replaced by the corresponding α5 sequence against which the anti-α5 antibody was raised (see Fig 6). In Fig.10 Panels A-C represent α5S23a staining, panels D-F α5S24a staining on transfected HEK cells. In green the anti-α5 antibody is visible. The red channel depicts anti-FLAG antibodies which recognize the N-terminal FLAG tag of the chimeric subunit (see Fig. 6). In yellow the overlay of these two channels is shown. Note that only successfully transfected cells are stained, while all surrounding non-transfected cells show very little background. We can therefore conclude, that the two new antibodies can selectively stain for the α5 subunit in transfected HEK-293 cells, but note that α5S24a emitted a weaker signal than the α5S23a antibody.

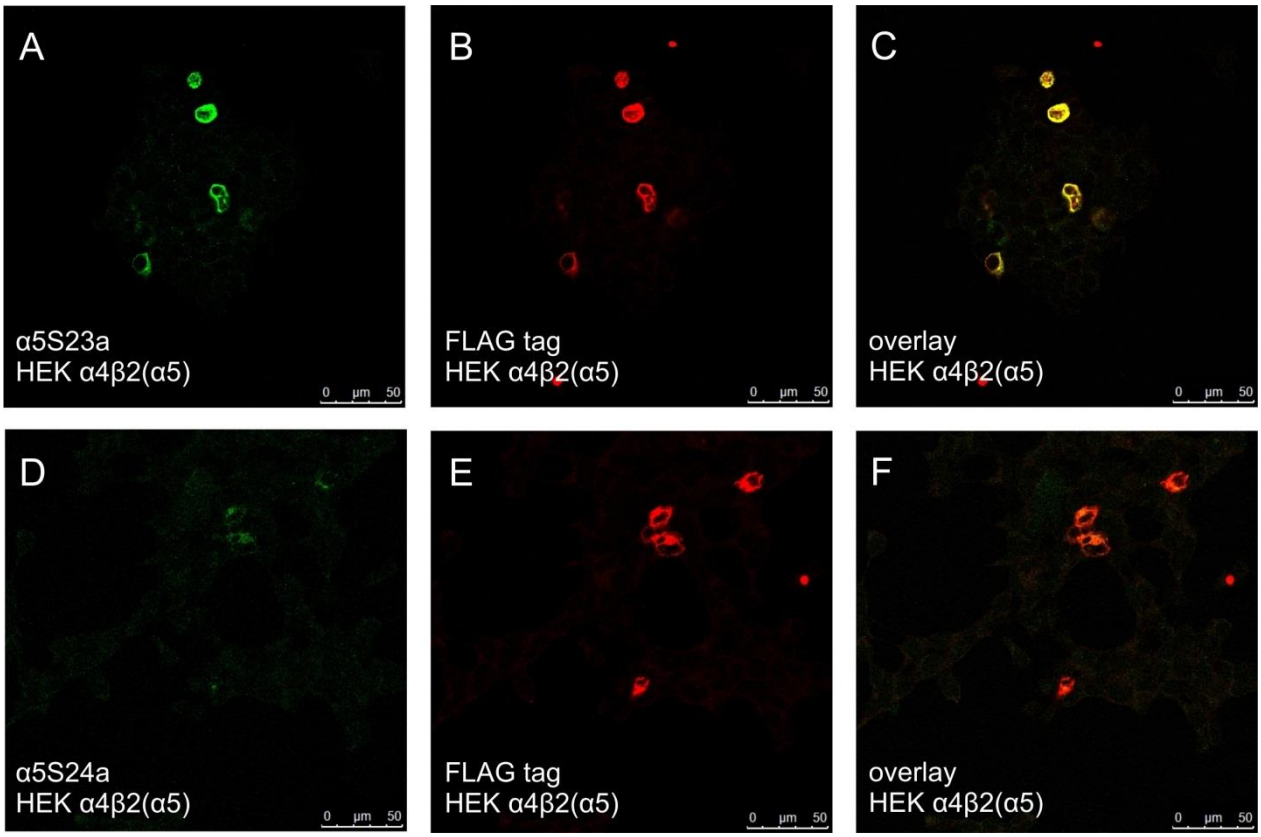

Figure 10 Immunocytochemicalstaining of the new rabbit S23a and S24a α5-antibodies on transfected HEK-293 cells | HEK-293 cells transfected with α4 and a chimeric β2 subunit (the intracellular loop of β2 was replaced with the homologous α5 region against which the anti-α5 antibodies were raised) were stained with the anti-α5 antibodies S23a (A) and S24a (D) shown in green as well as with a FLAG antibody (panels B and E) shown in red according to the protocol described in 2.8. (C) and (E). The transfected α5 construct expressed an extracellular N-terminal FLAG tag which was used to distinguish transfected from untransfected HEK cells which served as a negative control. Rabbit antibodies were detected with Alexa rabbit 488 and FLAG antibodies were detected with Alexa mouse 568 antibodies. Images were obtained using a Leica TCS SP5 confocal fluorescence microscope.

3.3.2 Rabbit antibodies α5S23a and α5S24a on primary cell cultures

Again further testing was conducted to assess whether the antibodies also find their antigen in native tissue. Therefore wild-type and α5-knockout SCGs were cultured and investigated immunocytochemically. On Fig. 11 panels A-D α5S23a was tested on neurons cultivated from wild-type (panels B and C) and α5-knockout (panels A and D) SCG. Panels E-H of Fig.11 show the staining of α5S24a on wild-type (panels F and H) and α5-knockout tissue (panels E and G). The anti-α5 antibody is shown in green and the anti-Actin antibody is shown red. There is no significant difference in staining intensity or pattern between wild-type and knockout tissue, indicating poor specificity of these antibodies in native tissue.

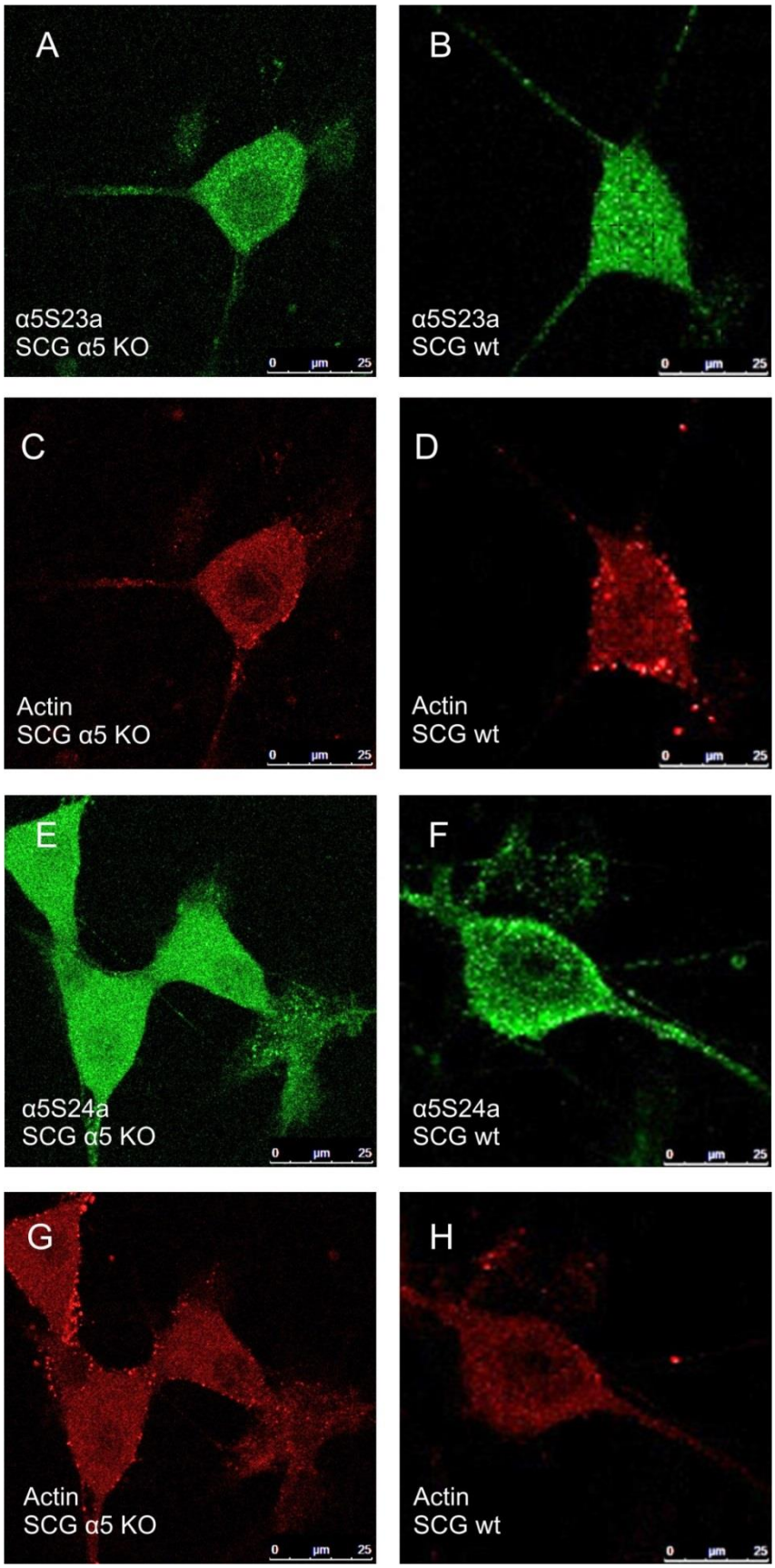

Figure 11 Immunocytochemical staining of neurons isolated from wild type and α5-knockout mice SCGs|
SCG cells of P3-P6 mice were cultured until DIV3-6 and then stained with the new anti-α5 antibodies S23a and S24a as described in
Panels C,D,G,H: stainings using an anti-actin- antibody
panels A, B: stainings using the a5S23a antibody
panels E, F: stainings using the a5S24a antibody
Panels A,C,E,G: neurons isolated from wild-type mice
Panels B,D,F, H: neurons isolated from knock-out mice

3.3.3 Guinea-pig anti-α5 antibodies S35, S36, S37 and S38 on heterologous tissue

The guinea-pig anti-α5 antibodies were also used to stain transfected HEK-293 cells.

Figures 12, 13, 14 and 15 show stainings of transfected HEK-293 cells with the guinea-pig antibodies S35, S36, S37 and S38 respectively. Panels A and D show α4β2(α5) transfected HEK cells (containing the α5 sequence) stained with the α5S35 antibody in blue and with the anti-FLAG antibody in red. Panel B and E show α4β2 transfected HEK cells stained with the α5S35 antibody in blue and α4S26 in green. This acts as a negative control for α5 as it ensures general transfection and expression of subunits detected by the anti-α4 antibody. Panels C and F are a similar control to further investigate the α5 specificity. α5S35 is shown in blue and β4S05 in green binding on α3β4 transfected HEK cells. α5S35 specifically binds its α5 antigen in transfected HEK cells. The well-characterized anti- β4 –antibody was used to stain α3β4 transfected HEK-293 cells as positive control.

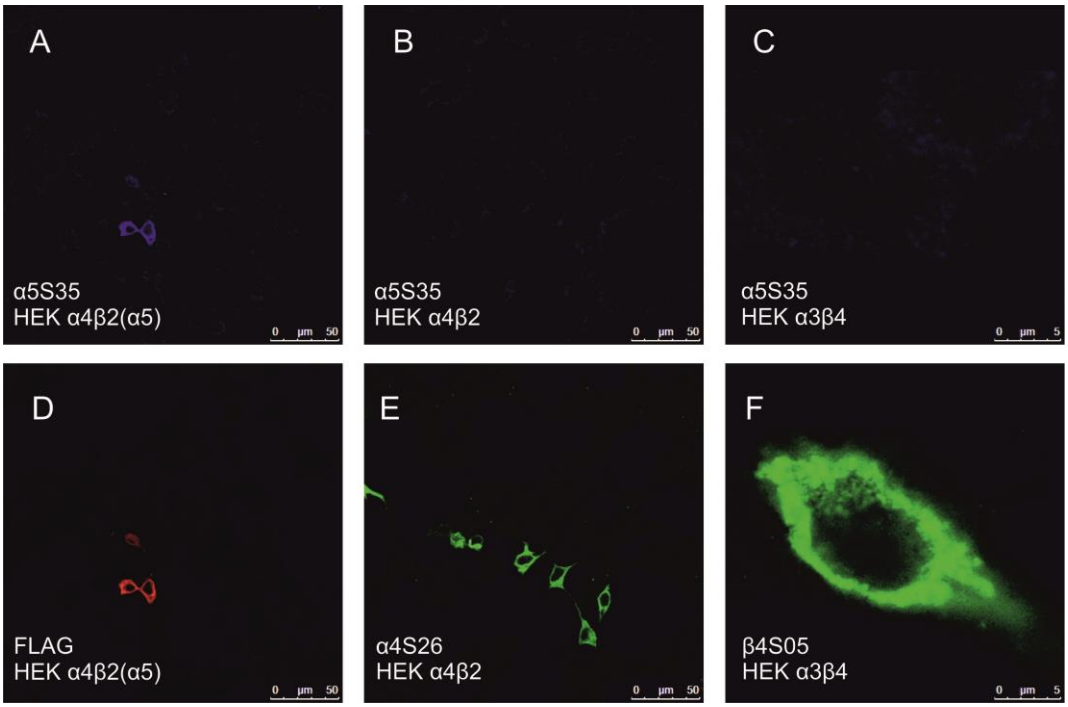

Figure 12 Immunocytochemical staining of guinea-pig S35 α5-antibody on transfected HEK-293 cells | HEK-293 cells transfected with α4 and altered chimeric β2 subunit (the intracellular loop of β2 was replaced with the homologous α5 region against which the anti-α5 antibodies were raised) were stained with (A) the anti-α5 antibody S35 shown in blue as well as (D) with a FLAG antibody shown in red. The transfected α5 construct expressed an extracellular N-terminal FLAG tag which was used to distinguish transfected from untransfected HEK cells which served as a negative control. HEK-293 cells transfected with α4 and β2 nAChR subunits were stained with (B) the anti-α5 antibody S35 shown in blue as well as (E) with a rabbit α4 antibody shown in green. HEK-293 cells transfected with α3 and β4 nAChR subunits were stained with (C) the anti-α5 antibody S35 shown in blue as well as (F) with a rabbit β4 antibody shown in green. Panels B and C served as additional negative controls. Guinea pig antibodies were detected with Alexa goat anti-guinea pig 647, rabbit antibodies were detected with Alexa rabbit 488 and FLAG antibodies were detected with Alexa mouse 568 antibodies. Images were obtained using a Leica TCS SP5 confocal fluorescence microscope. Stainings were performed as described in 2.8.

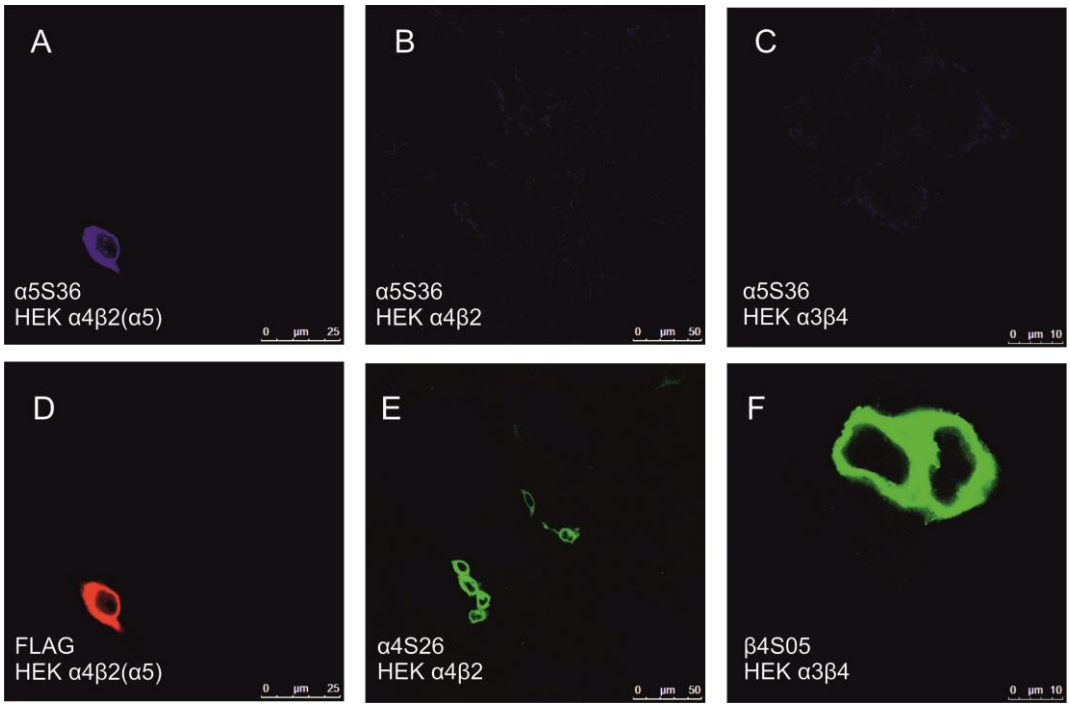

Figure 13 Immunocytochemical staining of guinea-pig S36 α5-antibody on transfected HEK-293 cells | HEK-293 cells transfected with α4 and a chimeric β2 subunit (the intracellular loop of β2 was replaced with the homologous α5 region against which the anti-α5 antibodies were raised) were stained with (A) the anti-α5 antibody S36 shown in blue as well as (D) with a FLAG antibody shown in red. The transfected α5 construct expressed an extracellular N-terminal FLAG tag which was used to distinguish transfected from untransfected HEK cells which served as a negative control. HEK-293 cells transfected with α4 and β2 nAChR subunits were stained with (B) the anti-α5 antibody S36 shown in blue as well as (E) with a rabbit α4 antibody shown in green. HEK-293 cells transfected with α3 and β4 nAChR subunits were stained with (C) the anti-α5 antibody S36 shown in blue as well as (F) with a rabbit β4 antibody shown in green. Panels B and C served as additional negative controls. Guinea pig antibodies were detected with Alexa goat anti-guinea pig 647, rabbit antibodies were detected with Alexa rabbit 488 and FLAG antibodies were detected with Alexa mouse 568 antibodies. Images were obtained using a Leica TCS SP5 confocal fluorescence microscope. Stainings were performed as described in 2.8.

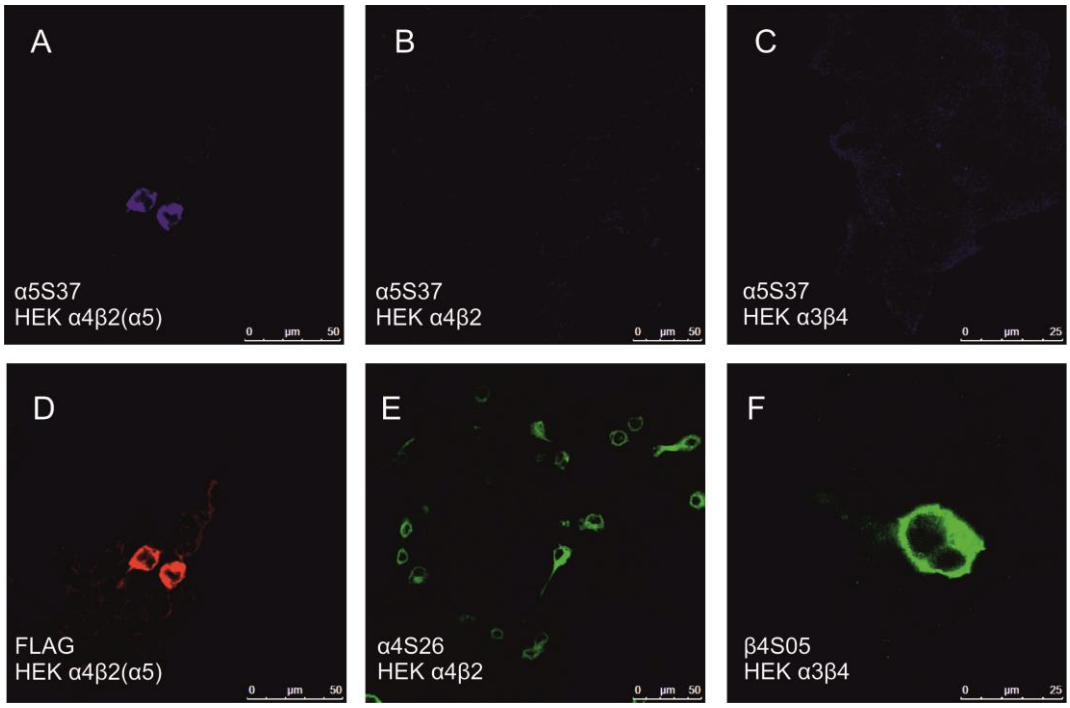

Figure 14 Immunocytochemical staining of guinea-pig S37 α5-antibody on transfected HEK-293 cells | HEK-293 cells transfected with α4 and a chimeric β2 subunit (the intracellular loop of β2 was replaced with the homologous α5 region against which the anti-α5 antibodies were raised) were stained with (A) the anti-α5 antibody S37 shown in blue as well as (D) with a FLAG antibody shown in red. The transfected α5 construct expressed an extracellular N-terminal FLAG tag which was used to distinguish transfected from untransfected HEK cells which served as a negative control. HEK-293 cells transfected with α4 and β2 nAChR subunits were stained with (B) the anti-α5 antibody S37 shown in blue as well as (E) with a rabbit α4 antibody shown in green. HEK-293 cells transfected with α3 and β4 nAChR subunits were stained with (C) the anti-α5 antibody S37 shown in blue as well as (F) with a rabbit β4 antibody shown in green. Panels B and C served as additional negative controls. Guinea pig antibodies were detected with Alexa goat anti-guinea pig 647, rabbit antibodies were detected with Alexa rabbit 488 and FLAG antibodies were detected with Alexa mouse 568 antibodies. Images were obtained using a Leica TCS SP5 confocal fluorescence microscope. Stainings were performed as described in 2.8.

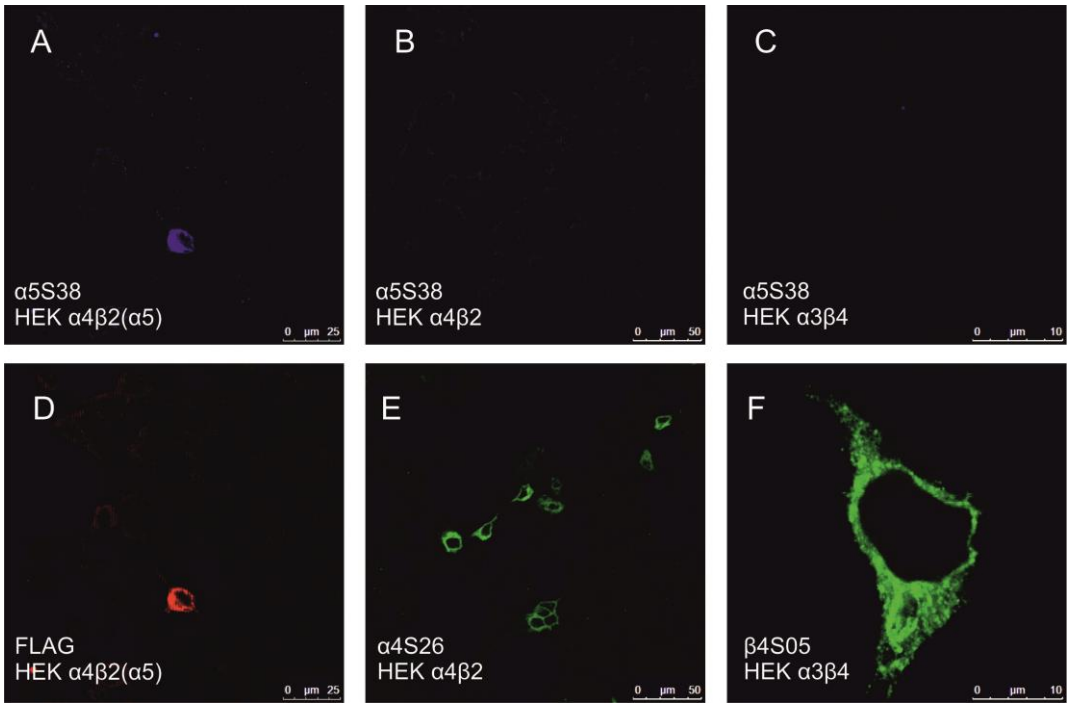

Figure 15 Immunocytochemical staining of guinea-pig S38 α5-antibody on transfected HEK-293 cells | HEK-293 cells transfected with α4 and a chimeric β2 subunit (the intracellular loop of β2 was replaced with the homologous α5 region against which the anti-α5 antibodies were raised) were stained with (A) the anti-α5 antibody S38 shown in blue as well as (D) with a FLAG antibody shown in red. The transfected α5 construct expressed an extracellular N-terminal FLAG tag which was used to distinguish transfected from untransfected HEK cells which served as a negative control. HEK-293 cells transfected with α4 and β2 nAChR subunits were stained with (B) the anti-α5 antibody S38 shown in blue as well as (E) with a rabbit α4 antibody shown in green. HEK-293 cells transfected with α3 and β4 nAChR subunits were stained with (C) the anti-α5 antibody S38 shown in blue as well as (F) with a rabbit β4 antibody shown in green. Panels B and C served as additional negative controls. Guinea pig antibodies were detected with Alexa goat anti-guinea pig 647, rabbit antibodies were detected with Alexa rabbit 488 and FLAG antibodies were detected with Alexa mouse 568 antibodies. Images were obtained using a Leica TCS SP5 confocal fluorescence microscope. Stainings were performed as described in 2.8.

3.3.4 Guinea-pig anti-α5 antibodies S35, S36, S37 and S38 on primary SCG cultures

Similar to the rabbit antibodies also guinea-pig antibodies were tested in native tissue. Therefore primary wild-type and various knockout SCG cultures were stained immunocytochemically. We stained wild-type, α5-knockout, α5α7β2-knockout and α5α7β4 knockout SCGs, as those together with α4 are the only nAChR subunits found in the SCG (David *et al.*, 2010). Since α4 is only expressed in fresh cultures of very young animals, the DIV6 stainings exclude cross-reaction with the α4-subunit (Scholze *et al.*, 2011). Figures 16, 17, 18 and 19 show SCG cultures of the previously mentioned genotypes stained with the guinea-pig antibodies S35, S36, S37 and S38 respectively.

The stainings show unspecific binding of the guinea pig anti-a5 antibodies. The most probable reason for unspecific stainings are cross-reactions with other nAChR subunits, but with the use of the triple knockout genotypes we can exclude this possibility.

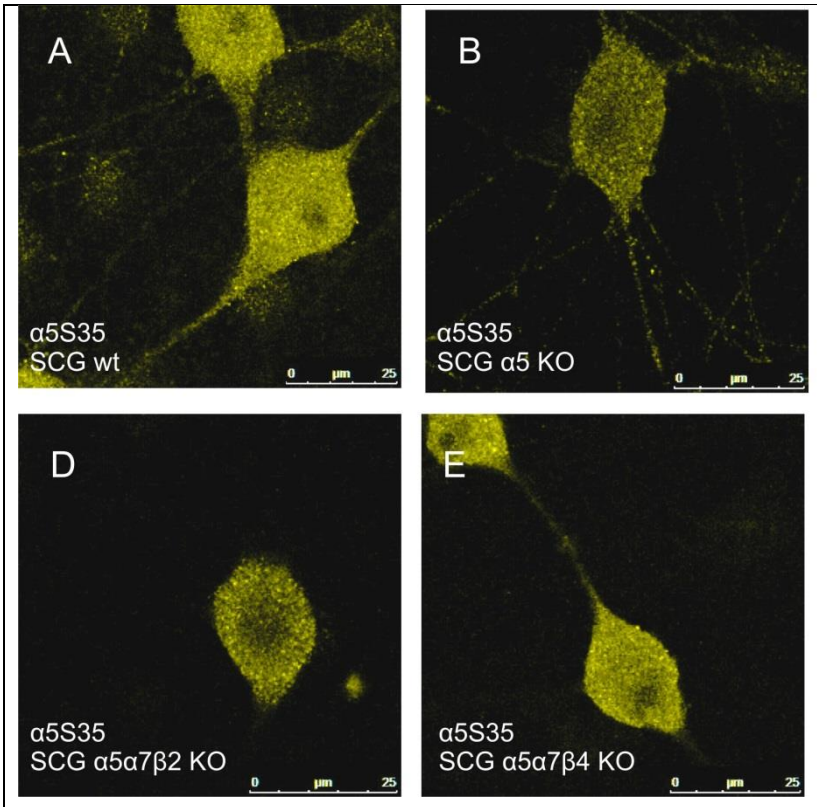

Figure 16 Immunocytochemistry staining of guinea-pig S35 α5-antibody on various mouse genotype SCGs | The guinea-pig ant-α5 antibody S35, shown in yellow was used to stain (A) SCG cells of P3-P6 wild type mice cultured until DIV3-6; (B) SCG cells of P3-P6 α5 knockout mice cultured until DIV3-6; (C) SCG cells of P3-P6 α5α7β2 triple knockout mice cultured until DIV3-6; (D) SCG cells of P3-P6 α5α7β4 triple knockout mice cultured until DIV3-6. Guinea pig antibodies were detected with Alexa goat anti-guinea pig 647. Images were obtained using a Leica TCS SP5 confocal fluorescence microscope. Stainings were done as described in 2.8.

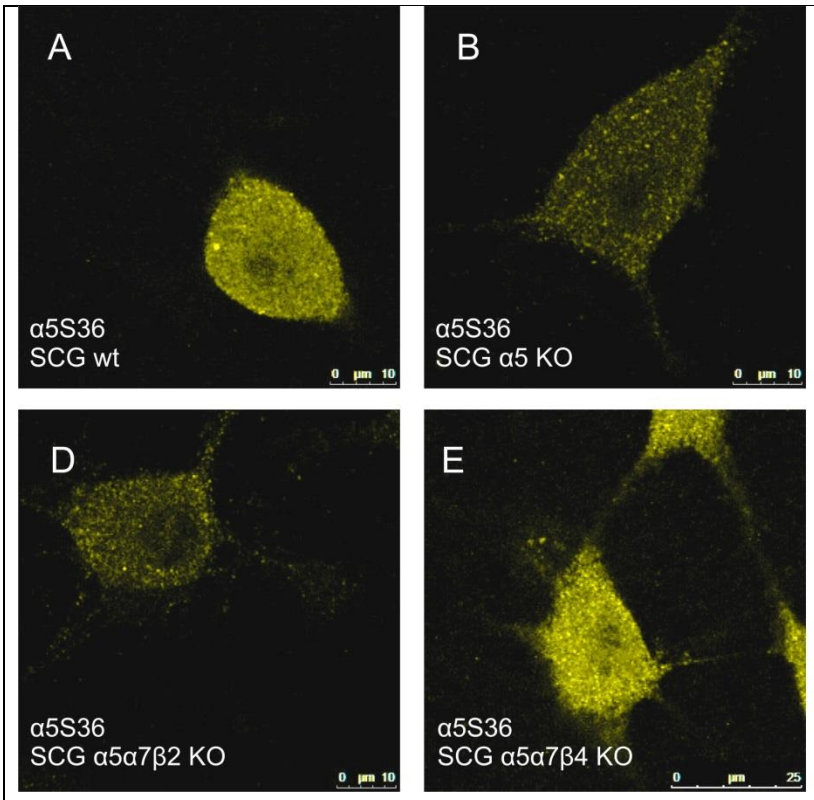

Figure 17 Immunocytochemistry staining of guinea-pig S36 α5-antibody on various mouse genotype SCGs | The guinea-pig anti-α5 antibody S35, shown in yellow for better contrast, was used to stain (A) SCG cells of P3-P6 wild type mice cultured until DIV3-6; (B) SCG cells of P3-P6 α5 knockout mice cultured until DIV3-6; (C) SCG cells of P3-P6 α5α7β2 triple knockout mice cultured until DIV3-6; (D) SCG cells of P3-P6 α5α7β4 triple knockout mice cultured until DIV3-6. Guinea pig antibodies were detected with Alexa goat anti-guinea pig 647. Images were obtained using a Leica TCS SP5 confocal fluorescence microscope. Stainings were done according to the protocol described in 2.8.

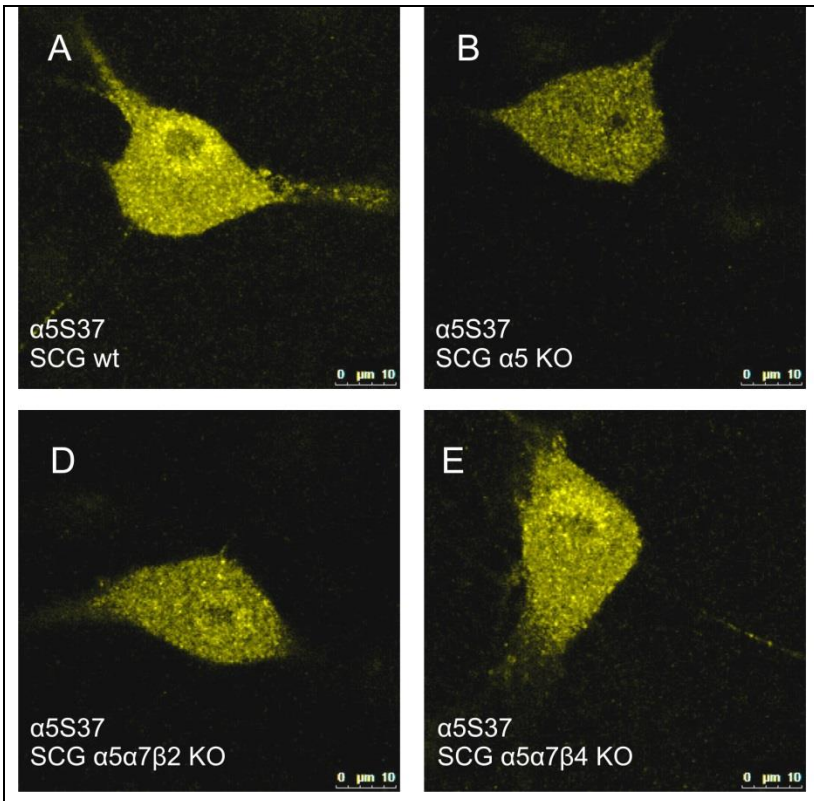

Figure 18 Immunocytochemistry staining of guinea-pig S35 α5-antibody on various mouse genotype SCGs | The guinea-pig anti-α5 antibody S35, shown in yellow for better contrast, was used to stain (A) SCG cells of P3-P6 wild type mice cultured until DIV3-6; (B) SCG cells of P3-P6 α5 knockout mice cultured until DIV3-6; (C) SCG cells of P3-P6 α5α7β2 triple knockout mice cultured until DIV3-6; (D) SCG cells of P3-P6 α5α7β4 triple knockout mice cultured until DIV3-6. Guinea pig antibodies were detected with Alexa goat anti-guinea pig 647. Images were obtained using a Leica TCS SP5 confocal fluorescence microscope. Stainings were done according to the protocol described in 2.8.

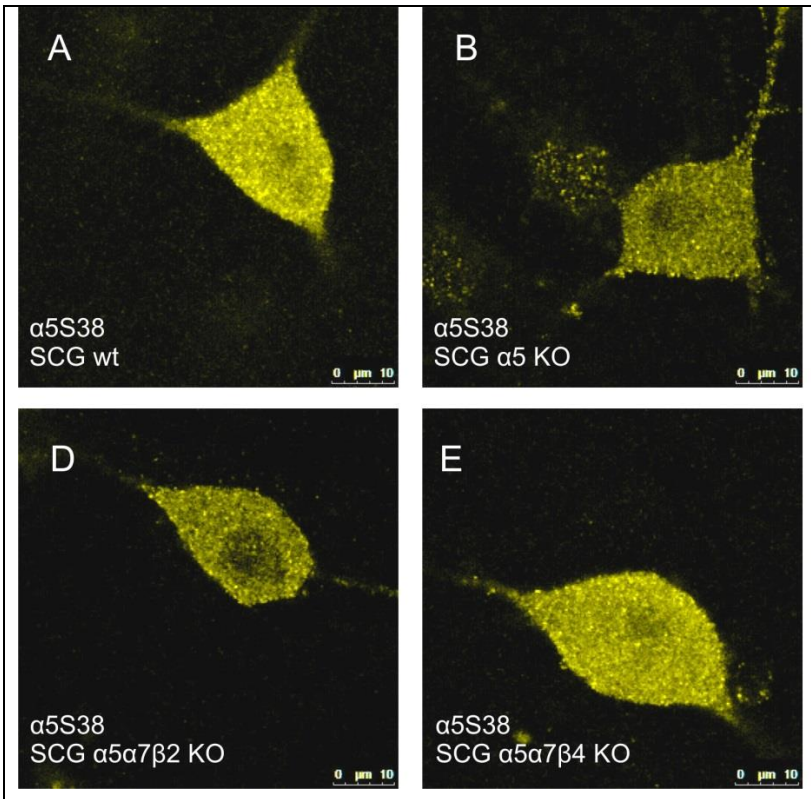

Figure 19 Immunocytochemistry staining of guinea-pig S35 α5-antibody on various mouse genotype SCGs | The guinea-pig ant-α5 antibody S35, shown in yellow for better contrast, was used to stain (A) SCG cells of P3-P6 wild type mice cultured until DIV3-6; (B) SCG cells of P3-P6 α5 knockout mice cultured until DIV3-6; (C) SCG cells of P3-P6 α5α7β2 triple knockout mice cultured until DIV3-6; (D) SCG cells of P3-P6 α5α7β4 triple knockout mice cultured until DIV3-6. Guinea pig antibodies were detected with Alexa goat anti-guinea pig 647. Images were obtained using a Leica TCS SP5 confocal fluorescence microscope. Stainings were done according to the protocol described in 2.8

3.3.5 Guinea-pig anti-α5 antibodies S35, S36, S37 and S38 on mouse brain habenula kryoslides

The final test was to investigate whether the new guinea-pig α5 antibdies could stain native anatomical structures. Therefore a region was chosen which is known for expressing detectable amounts of α3, α4, β4 as well as α5 (Gotti *et al.*, 2006; Putz *et al.*, 2008) namely the medial Habenula. Kryosections of mouse brains were subjected to immunohistochemical staining. Panel A of Fig. 20 shows the positive control in which Actin is colored red and β4 in green. The symmetrical green area detected by the rabbit anti-β4 antibody marks the medial habenula which ensures that the kryosections were made in the right area of the brain. Panels B –E show the binding of the guinea-pig antibodies S35-S36 in consecutive brain slices. No specific staining pattern could be detected.

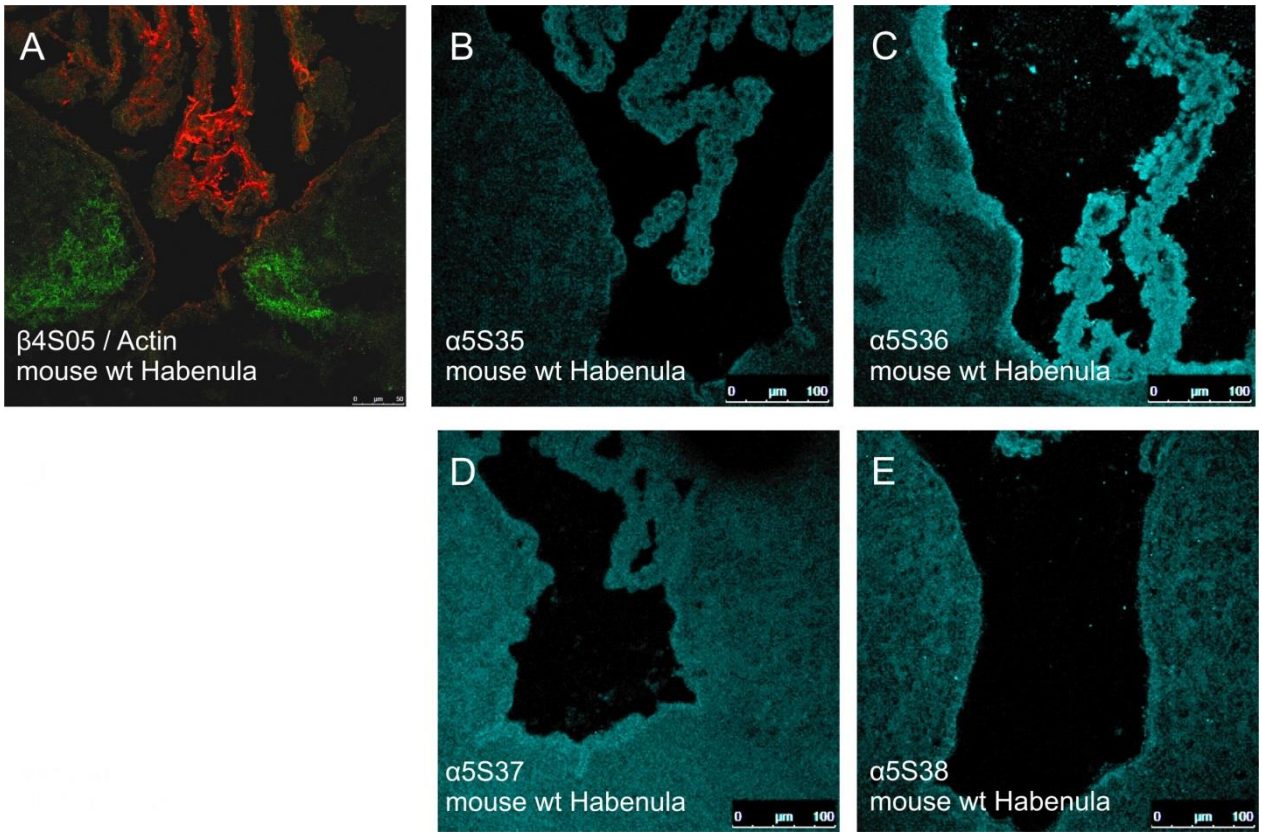

Figure 20 Immuncytohistochemical staining of guinea pig anti-α5 antibodies on cryosections from the medial habenula in the brain of 18 days old wt mice | 15µm cryosections of the medial habenula of P18 wild-type mice were immunocytohistochemically stained using (A) β4 and Actin antibodies as a positive control (B) guinea-pig S35 anti-α5 antibody (C) guinea-pig S36 anti-α5 antibody (D) guinea-pig S37 anti-α5 antibody and (D) guinea-pig S38 anti-α5 antibody. Guinea pig antibodies were detected with Alexa goat anti-guinea pig 647, rabbit antibodies were detected with Alexa rabbit 488 and FLAG antibodies were detected with Alexa mouse 568 antibodies. Images were obtained using a Leica TCS SP5 confocal fluorescence microscope. Cryosections and stainings were created according to Material&Methods 2.9 respectively 2.10.

3.4 IPN subunit composition

Nicotinic acetylcholine receptors from the IPN from wild-type, α5-knockout, β2-knockout and β4-knockout mice were immunoprecipitated with antibodies against the α2, α3, α4, α5, α6, β2 and β4 subunits. α3, α4, β2 and β4 are the most abundant nAChR subunits in the IPN, whereas α2, α3 and α6 are the least expressed subunits. In the wild-type IPN the overall receptor concentration was 27,13 ± 2,05 fmol/IPN (285,45 ± 27,91 fmol/mg lysate protein, n=3). The single subunit concentrations are shown in Table 6. Information about the receptor co-assemblies can be drawn from the changes found between the receptor levels of a given subunit in the brains from WT and KO mice.

	fmol/IPN	fmol/mg lysate protein
α2	3.08 ± 0.19	39.15 ± 3.18
α3	13.66 ± 0.89	174.16 ± 17.35
α4	11.04 ± 0.96	139.40 ± 8.40
α5	2.44 ± 0.29	30.57 ± 1.32
α6	0.77 ± 0.05	9.84 ± 0.58
β2	14.51 ± 1.01	183.87 ± 13.20
β4	12.62 ± 1.23	161.37 ± 21.77

Table 6 wild-type IPN subunits

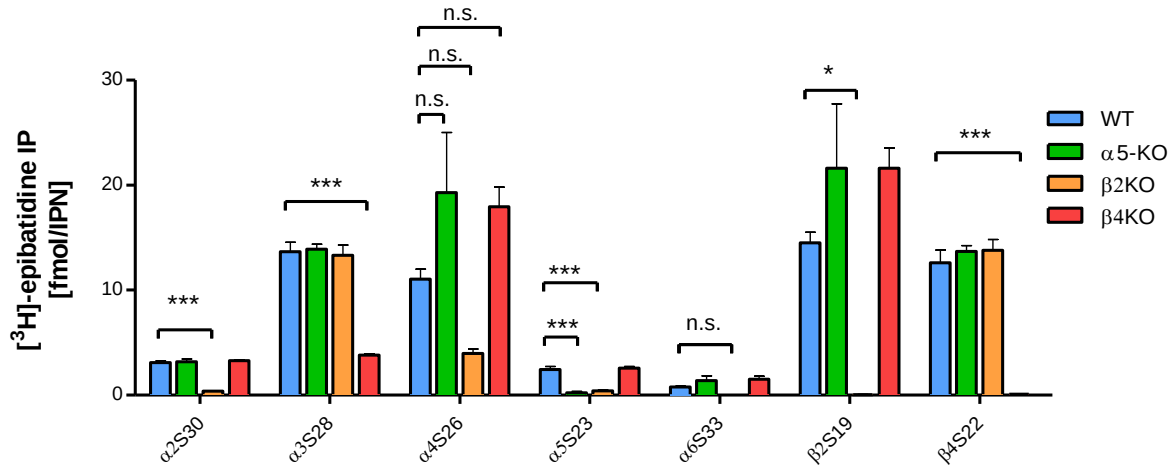

Figure 21 Subunit levels in the IPN from various P18 mouse genotypes as detected by immunoprecipitation using subunit specific nAChR antibodies | (A) and (B) solubilized IPN from P18 wild type mice were labeled with 1nM [^{3}H] Epibatidine and immunoprecipitated using α2, α3, α4, α5, α6, β2 and β4 antibodies. The results are shown as the absolute amount of precipitated nAChR subunit in fmol/mg lysate. Each colored bar represents a mouse genotype. Wild-type is diagrammed in blue, α5-knockout in green, β2-KO in orange and β4-KO in red. The data shows mean ±SEM of three independent experiments whereas every datapoint was measured in duplicates. Column data were compared using one-way ANOVA followed by Dunnett's multiple comparison test. Significantly different from WT with * $p < 0.05$, ** $p < 0.005$, *** $p < 0.001$. n.s.: not significant ($p > 0.05$).

4 Discussion

4.1 Antibody characterization using IP

Immunoprecipitation is a long and extensively used technique in our lab. It is easy to use and the method of choice to assess the quality of antibodies. Since commercially available antibodies mainly lack specificity a rigorous quality check is needed for antibody specification. Immunoprecipitation in combination with knock-out mouse lines is therefore a powerful tool.

4.1.1 Rabbit antibodies α5S23a and α5S24a on heterologous tissue

In HEK-293 cells transfected with the α4-subunit and a chimeric β2-subunits containing the α5 sequence loop, all of the receptors were precipitated with the old as well as with the two new anti-α5 antibodies. In transfected HEK cells that expressed other nAChR subunits no precipitation of α5 was detected. In heterologous tissue the new antibodies α5S23a and α524a show the same excellent specificity and efficacy as the predecessor α5S23.

However heterologous cell systems differ from the native cell environment. HEK-293 cells are immortalized embryonic kidney cells, which are able to express introduced DNA. We transfected these cells with nAChR-subunit cDNA in pCI expression vectors through calcium-phosphate transfection (Jordan *et al.*, 1996). As the host system is human and the introduced DNA is from mouse, posttranslational modifications could eventually differ. The most striking difference however is the expression level, which is much higher in transfected HEK cells than in neuronal tissue. Therefore we also needed to perform tests in native tissue.

4.1.2 Rabbit antibodies α5S23a and α5S24a on native tissue

As already mentioned a heterologous system has some drawbacks and can only be the first step in the specification of an antibody. Therefore as a next step we used native neuronal tissue for testing the newly generated antibodies using immunoprecipitation. We chose to use SCG and IPN, since they are brain regions where α5-subunits are expressed at exceptionally high levels (see Fig 4).

The SCG is the uppermost ganglion of the paravertebral ganglia of the sympathetic nervous system. It innervates peripheral targets like glands and smooth muscles and thereby controls involuntary body functions like heart rate and sweating (Purves *et al.*, 1988). In 18days old mice it is approximately the size of 1mm^2 and the adult SCG contains about 10,000 neurons. (Wright & Smolen, 1987).

The fact that we find exceptionally high a5-levels in SCG is in compliance with other studies, which report ~34% α5 subunit content in rat SCG (Mao *et al.*, 2006; Mao *et al.*, 2008).

We directly compared the already well characterized α5S23 antibody (David *et al.*, 2010) with the newly generated anti-α5 antibodies S23a and S24a in three independent IP experiments. The new antibodies were inferior to the "old" S23 antibody as they only precipitated a third of the α5 nAChR subunit population.

Another native tissue we chose was the interpeduncular nucleus (IPN). The IP has the second highest amount of α5 nAChR subunits according to data from our lab (see Fig. 4). The IPN is located in the center line of the ventral midbrain and is an unpaired nucleoid structure. It receives solely input from the medial habenula via the fasciculus retroflexus and projects among other locations to the ventral and dorsal tegmental areas. It therefore plays a key role in addiction and pathways and has the highest levels of choline acetyltransferase (ChAT) in the brain (Klemm, 2004; Kobayashi *et al.*, 2013; Leslie *et al.*, 2013).

In wild type IPN tissue α5S23 precipitated 24,8 ± 3,7 fmol/mg lysate protein, the new purified antibodies α5S23a 11,3 ± 1,0 fmol/mg lysate protein and α5S24a 11,3 ± 0,6 fmol/mg lysate protein (see Fig. 9, Panels A & B). Other findings suggest 52,0 ±5,7 fmol/mg protein, which is double the amount found by us (Grady *et al.*, 2009). However the amount of nAChRs precipitated by the newly generated anti-α5 antibodies is only halve of the reference α5S23.

In α5-knockout IPN none of the anti-α5 antibodies generated at our lab show precipitation, which underlines the specificity of our antibodies (see Fig.9, Panels C & D).

Although the outstanding specificity of the antibodies it remains unclear why they precipitate other amount of nAChR in native tissue despite having the same concentration.

One could speculate that since the antibodies were raised against a denatured sequence of the antigen (MBP-fusion protein in guanidine-HCl/8M Urea) they could not detect their proper antigen in the native folded state.

The strength of a single non-covalent antibody – antigen binding is called affinity, whereas the multiplicity of such non-covalent bindings from multiple antibodies to an epitope is called avidity. It is possible that the affinity was weaker or that the resulting binding complex is not as effective as it is with the formerly described antibodies. Following this thought, the used concentration of S23a and S24a antibody was too low to effectively bind the same antigen amounts.

Another theory could be that an intracellular protein or even a complex not present in HEK cells associate with the loop-binding region of the receptor thereby blocking antibody binding.

4.2 Antibody characterization using immunocytochemistry in native tissue

Since the new antibodies are not suitable for IP, we wanted to know, if they could be used for immunocytochemistry:

First, we investigated the newly synthesized antibodies α5S23a and α5S24a in transfected HEK-293 cells. Our findings, as shown in Figure 10 show that the staining signal of both of these new anti-alpha-antibodies is very specific although α5S24a gives a slightly weaker signal than the other antibodies at the same concentration used. Again we also tested the antibodies on native tissue (see Fig. 11 A-D)

Unfortunately, in primary neuronal cell culture, there is no significant difference in staining intensity or pattern between wild-type and knockout tissue. Also the nuclei is often stained which should not be the case as nicotinic receptors are made in the ER and brought to the plasma-membrane by COPII particles. At the membrane they can be endocytosed to finally end up in a lysosome where they are degraded or recycled (Colombo *et al.*, 2013). It is the most likely scenario that the epitope of the anti-α5 antibodies cross-react with other cell proteins, because α5-knockout mice do not express the α5 subunit at all which also was proven in our lab by IP-experiments from α5-knockout mice.

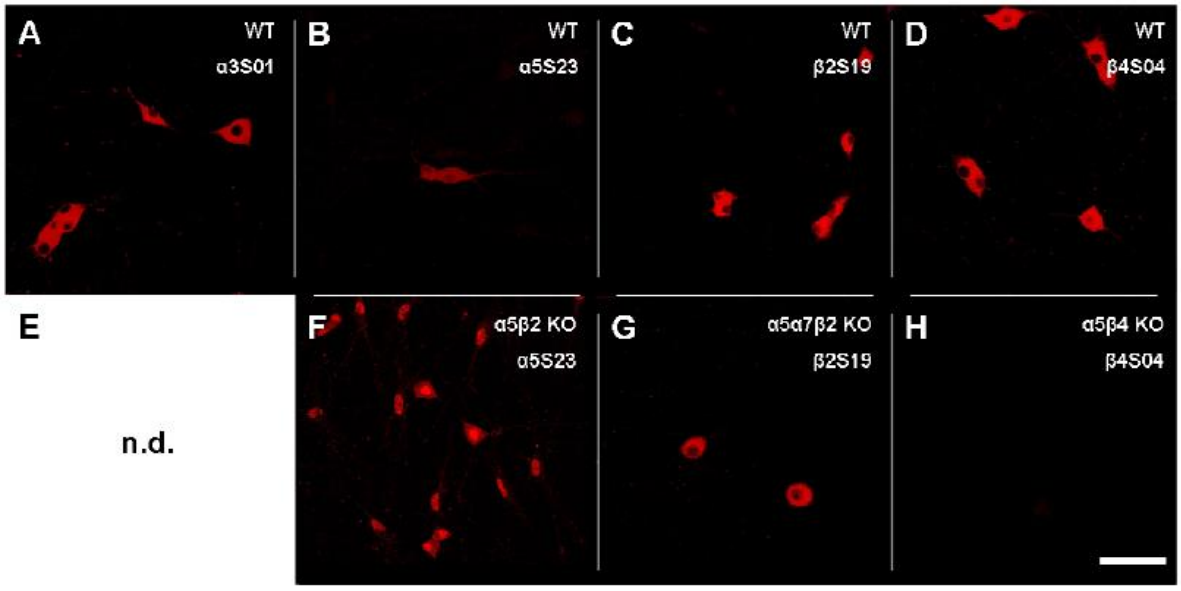

Figure 22 Immuncytochemistry staining of P3 mouse SCGs | Panels B and C show αS23 binding unspecifically on wild-type and α5 knockout tissue. (taken from Doctoral Thesis of Reinhard David, 2011)

In 2011, Reinhard David reported a similar finding with an unspecific cell nuclear staining in his doctoral thesis, where he described the first α5S23 antibody (see Fig. 22). To improve the staining the fixation condition of the tissue were modified, since it is a very important point of making the epitope accessible for the antibody respectively letting the antibody diffuse to its antigen (Watanabe *et al.*, 1998). This is in particular important because the anti-α5 antigen on the nAChR is located at the intracellular loop between the transmembrane domains M3 and M4 (see Fig. 6 and Fig. 2). I therefore altered the duration of PFA fixation from 10 to 20 minutes and instead of fixation at room temperature, fixation on ice was conducted. Additionally methanol instead of PFA but none of the variation yielded improved staining results although methanol staining resulted in better resolution microscope images of the cell cytoskeleton. In order to reduce background staining, the compisiton of the blocking solutions were varied from 3% NDS in 0,2% Triton/PBS to 2,5% BSA in 0,2% Triton/PBS and Pierce Superblock Blocking Puffer (http://www.piercenet.com/product/superblock-blocking-buffers) in order to provide more stringent conditions avoiding unspecific binding. The different blocking solutions did not influence the staining at all, suggesting that not unspecific staining but cross-reaction with an unknown nAChR associated protein leads to the observed stainings.

4.2.1 Guinea-pig anti-anti-α5 antibodies S35, S36, S37 and S38 on heterologous tissue

We also generated antibodies in a different species. If successful this would enable us to perform double stainings of e.g. a rabbit anti-β4 and a guinea-pig anti- α5.

Fig. 12-15 show the guinea pig α5S35-S38 antibody staining on different HEK-293 cells. Here we successfully showed a triple staining of guinea-pig, rabbit, and mouse antibodies. The guinea-pig antibodies α5S35 – α5S38 all specifically bind their α5 antigen in transfected HEK cells. For the positive control an anti-β4 antibody was used, which was extensively characterized in the doctoral thesis of Reinhard David and proved to work perfectly in IP, Immunocytochemistry and Western Blot.

4.2.2 Guinea-pig anti-anti-α5 antibodies S35, S36, S37 and S38 on primary cell cultures

Fig. 16 - 19 show the guinea pig α5S35-S38 staining of primary neurons cultured from wild-type, α5-knockout, α5α7β2-knockout and α5α7β4 knockout SCGs. Like the rabbit antibodies in native tissue, the guinea-pig anti-α5 antibodies bind unspecifically and in the cell nuclei. To exclude a possible cross-reaction with one another different nAChR-subunit neurons from additional knock-out animals were testet. Since SCGs only express a small subset of nAChR-subunits, namely α3, α5, α7, β2, β4 (Putz *et al.*, 2008; David *et al.*, 2010) with the two additional knockout combinations α5α7β2 and α5α7β4 triple knockouts we could test all other occurring subunits. Since we still see cross-reactivity we assume that

our antibody cross-reacts with an independent still unknown protein. A BLAST research showed no sequence homology with other subunits, however since the antibodies were directed against denatured MBP-α5 sequence, there could be epitope-homologies in the native folded state.

4.2.3 Guinea-pig anti-α5 antibodies S35, S36, S37 and S38 on mouse brain habenula cryoslides

To test the guinea-pig anti-α5 antibodies in anatomical intact structures a region was chosen which is known for expressing detectable amounts of α3, α4, β2, β4 as well as α5 (Gotti *et al.*, 2006; Putz *et al.*, 2008; Scholze *et al.*, 2012) namely the medial Habenula. In panel A of Fig. 20 the medial Habenula can be seen, clearly defined by the region stained by the anti-β4 antibody shown in green. Actin, which is shown in red, spans the whole cell and was used as a landmark to navigate microscopically to the right structure and to have a comparable staining intensity. In Fig. 23 you see the previous staining work of our lab proving the functionality of the anti-β4 antibody in red with antibodies against vesicular acetylcholine transporter in green as a control. The good correlation of the staining in Fig.20 and 23 ensured that the kryoslides were made in the right section of the brain.

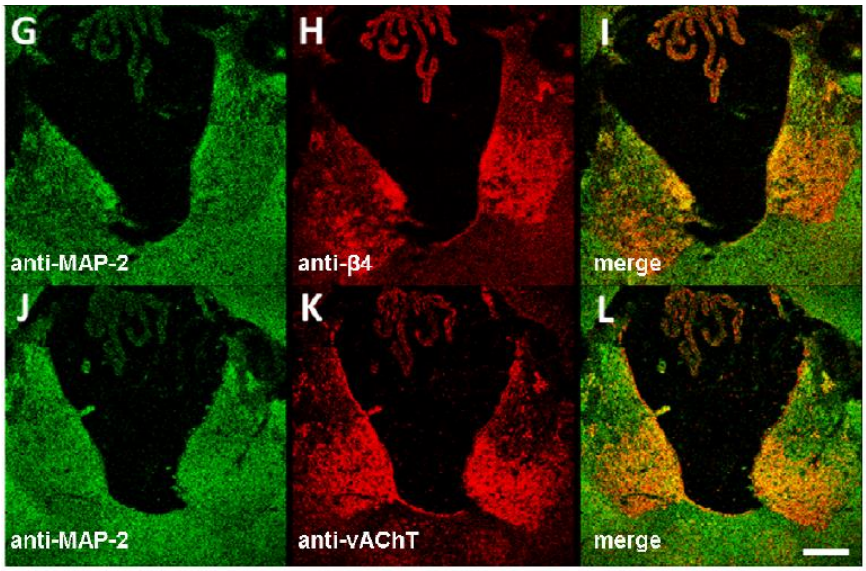

Figure 23 Immunohistochemical staining of the media Habenula | Reinhard David was able to visualize the medial habenula with anti-vAChT, an Anti-Vesicular Acetylcholine Transporter antibody and anti-β4 antiobdies from our lab (image taken from Doctoral Thesis of Reinhard David, 2011)

Although the medial Habenula was correctly cut in the cryoslices, the antibodies S35-S38 could not specifically bind their α5 antigen and show a homogeneous staining pattern. But as the staining of intact brain structures was expected to be more difficult than staining primary cell cultures, the unspecific staining result was not very surprising although cryosections provide the best antigen preservation

(Fischer *et al.*, 2008). However altering the perfusion fixation method was not tested but with weaker fixation methods especially for intracellular markers probably better results could have been obtained.

4.3 Mouse IPN nAChR subunit composition

Despite having no fully functional anti-α5 antibody working in immunohistochemistry and immunocytochemistry, the antibody a5S23 from our laboratory has proven its excellent performance in previous studies (David *et al.*, 2010; Scholze *et al.*, 2012; Beiranvand *et al.*, 2014). The a5S23 was already used in revealing the nAChR composition in the SCG (David *et al.*, 2010) and Habenula (Scholze *et al.*, 2012) and was now the tool to determine the nAChR composition of the IPN. The focus of our study were the α5 containing receptors in the IPN, as it is very rich in α5 and expresses receptors types which are very rarely expressed throughout the rest of the brain.

Fig. 21 not only unveils the wild-type subunit composition like seen in Table 6, but using knockout mice, information about the co-assembly of the subunits can be drawn. Although compensation mechanisms for knockout subunits were never discovered in SCG or Habenula (David *et al.*, 2010; Scholze *et al.*, 2012), these conclusions are only true if there is no up – or downregulation of other subunits as a compensation for the knockout subunit.

In wild-type mice the most abundant nAChR subunits in the IPN were α3, α4, β2 and β4, which was also reported by others (Grady *et al.*, 2009).

In the IPN of β4 knockout mice only the α3 subunit is significantly reduced from 13,7 ±0,9 in wild-type to 3,80± 0,1 fmol/IPN. From that we conclude that α3 mostly co-assembles with β4 subunits. This is in line with other findings that peripheral neurons of the medial habenula, medulla, pineal gland and retina mainly consist of α3β4 subunits but also contain accessory subunits (Jensen *et al.*, 2005; Gotti *et al.*, 2009).

In β2 knockout mice α2 subunit is significantly reduced from 3,1 ± 0,2 in the wild-type to 0,36 ± 0,03 fmol/IPN, α4 is significantly reduced from 11,04 ± 0,96 in the wild-type to 3,97 ± 0,41 fmol/IPN and the α5 subunit is significantly reduced from 2,44 ± 0,29 in the wild-type to 0,41 ± 0,06 fmol/IPN.

The α6 subunit count drops from wild-type 0,77 ± 0,05 fmol/IPN to 0,01 ±0,01 in β2 knockout IPN. This is not significant according to one way ANOVA statistics following Dunnett's Multiple comparison with n=3. But considering other data of our lab, which increased the number of measurements to n=5, the difference from β2 knockout to wild-type is significant. Furthermore the amount of α6 subunits in β2 knockout IPN is not significantly different from zero, suggesting that all α6 receptor co-assemble with β2. This is contradictory to other findings which detected no α6 at all in mouse IPNs (Grady *et al.*, 2009).

Taking only my data into account, the α5 subunit exclusively co-assembles with β2, because in β2 knockout IPN the α5 level drop to the same as in α5 knockout IPN. Moreover the β4 knockout has no significant or slightly observable effect on α5 levels. This agrees with other findings reporting that in the rat hippocampus, thalamus, cerebral cortex and the striatum the α5 subunit was found almost exclusively associated to β2 receptors specifically in α4 β2 α5 receptors (Mao *et al.*, 2008).

Overall these findings suggest that α2, α4, α5 and α6 co-assemble with β2 which is partially according to Grady et al where they found α2, α3 and α4 co-assembling with the β2 subunit including accessory subunits α5 and β3 and α3 co-assembles with β4 (Grady *et al.*, 2009).

4.4 Conclusion / Outlook

We successfully immunized rabbits and guinea-pigs with a modified α5-antigen construct. The animals produced polyclonal antibodies against that protein which were successfully purified by our lab. These antibodies were then characterized extensively.

The generated anti-α5 antibodies in rabbit and guinea-pig are able to precipitate their antigen in homologue tissue like transfected HEK-293 cells specifically and quantitatively.

The rabbit antibodies S23a and S24a are also able to precipitate their α5 antigen specifically in native tissue like SCG and IPN, but fail to do so quantitatively as they showed 30-50% less signal than the well characterized antibody α5S23a (David *et al.*, 2010). For the guinea pig anti-α5 antibodies no immunoprecipitation experiments were made because the yield of the animals was very low and immunoprecipitation needs quite large amounts of antibody in comparison with immunocytochemical methods.

The generated anti-α5 antibodies in rabbit and guinea-pig are able to stain homologue tissue like transfected HEK-293 cells with good specificity and also triple staining of transfected HEK-293 cells using detection of guinea-pig, rabbit and mouse antibody was conducted successfully.

However the antibodies fail when it comes to specifically stain native tissue like primary SCG cells or cryoslides of the mouse medial Habenula. This difficulty in recognizing the antigen specifically in native tissue can have several reasons like lack of epitope accessibility, epitope cross reaction and improper tissue preparation (Watanabe *et al.*, 1998; Schneider Gasser *et al.*, 2006; Lorincz & Nusser, 2008; Buchwalow *et al.*, 2011).

For future stainings, further modifications of the fixation methods and preservation of the antigen could lead to specific staining, as the antibody per se is able to specifically detect its antigen in non-native tissue. Since polyclonal antibodies are directed against random pieces of an epitope, simply a new immunization of animals could result in well performing antibodies. However the best approach getting an anti-α5 antibody that works in Immunoprecipitation, Immuncytocemistry as well as in Western Blot would be to alter the α5 sequence against which the immune system of the animals will be directed. An idea would be to split the epitope of the intracellular loop into two pieces, hoping to eliminate the cross-reactive sequence in at least one of the constructs, and look whether this yields better detection quality.

Another approach would be to generate monoclonal antibodies using Hybridoma cells. I experimented with existing Hybridoma cell cultures generated in 2002, but besides proliferating them in serum free media no successful binding experiments could be reported.

To further determine the subunit stoichiometry of the IPN sequential IP experiments would be necessary as done for the SCG or for the habenula (David *et al.*, 2010; Scholze *et al.*, 2012). With the help of the pre-clearing of specific subunits the actual corresponding co-assembling subunits could be unveiled.

5 References

Albuquerque, E.X., Pereira, E.F., Alkondon, M. & Rogers, S.W. (2009) Mammalian nicotinic acetylcholine receptors: from structure to function. *Physiological reviews*, **89**, 73-120.

Bailey, C.D., De Biasi, M., Fletcher, P.J. & Lambe, E.K. (2010) The nicotinic acetylcholine receptor alpha5 subunit plays a key role in attention circuitry and accuracy. *The Journal of neuroscience : the official journal of the Society for Neuroscience*, **30**, 9241-9252.

Beiranvand, F., Zlabinger, C., Orr-Urtreger, A., Ristl, R., Huck, S. & Scholze, P. (2014) Nicotinic acetylcholine receptors control acetylcholine and noradrenaline release in the rodent habenulo-interpeduncular complex. *British journal of pharmacology*, **171**, 5209-5224.

Bierut, L.J., Stitzel, J.A., Wang, J.C., Hinrichs, A.L., Grucza, R.A., Xuei, X., Saccone, N.L., Saccone, S.F., Bertelsen, S., Fox, L., Horton, W.J., Breslau, N., Budde, J., Cloninger, C.R., Dick, D.M., Foroud, T., Hatsukami, D., Hesselbrock, V., Johnson, E.O., Kramer, J., Kuperman, S., Madden, P.A., Mayo, K., Nurnberger, J., Jr., Pomerleau, O., Porjesz, B., Reyes, O., Schuckit, M., Swan, G., Tischfield, J.A., Edenberg, H.J., Rice, J.P. & Goate, A.M. (2008) Variants in nicotinic receptors and risk for nicotine dependence. *The American journal of psychiatry*, **165**, 1163-1171.

Boorman, J.P., Beato, M., Groot-Kormelink, P.J., Broadbent, S.D. & Sivilotti, L.G. (2003) The effects of beta3 subunit incorporation on the pharmacology and single channel properties of oocyte-expressed human alpha3beta4 neuronal nicotinic receptors. *The Journal of biological chemistry*, **278**, 44033-44040.

Buchwalow, I., Samoilova, V., Boecker, W. & Tiemann, M. (2011) Non-specific binding of antibodies in immunohistochemistry: fallacies and facts. *Scientific reports*, **1**, 28.

Cartaud, J., Benedetti, E.L., Cohen, J.B., Meunier, J.C. & Changeux, J.P. (1973) Presence of a lattice structure in membrane fragments rich in nicotinic receptor protein from the electric organ of Torpedo marmorata. *FEBS letters*, **33**, 109-113.

Champtiaux, N. & Changeux, J.P. (2004) Knockout and knockin mice to investigate the role of nicotinic receptors in the central nervous system. *Progress in brain research*, **145**, 235-251.

Champtiaux, N., Han, Z.Y., Bessis, A., Rossi, F.M., Zoli, M., Marubio, L., McIntosh, J.M. & Changeux, J.P. (2002) Distribution and pharmacology of alpha 6-containing nicotinic acetylcholine receptors

analyzed with mutant mice. *The Journal of neuroscience : the official journal of the Society for Neuroscience*, **22**, 1208-1217.

Chang, C.C. & Lee, C.Y. (1963) Isolation of Neurotoxins from the Venom of Bungarus Multicinctus and Their Modes of Neuromuscular Blocking Action. *Archives internationales de pharmacodynamie et de therapie*, **144**, 241-257.

Changeux, J.P. (2010) Nicotine addiction and nicotinic receptors: lessons from genetically modified mice. *Nature reviews. Neuroscience*, **11**, 389-401.

Charpantier, E., Barneoud, P., Moser, P., Besnard, F. & Sgard, F. (1998) Nicotinic acetylcholine subunit mRNA expression in dopaminergic neurons of the rat substantia nigra and ventral tegmental area. *Neuroreport*, **9**, 3097-3101.

Chinta, S.J. & Andersen, J.K. (2005) Dopaminergic neurons. *The international journal of biochemistry & cell biology*, **37**, 942-946.

Colombo, S.F., Mazzo, F., Pistillo, F. & Gotti, C. (2013) Biogenesis, trafficking and up-regulation of nicotinic ACh receptors. *Biochem Pharmacol*.

Cooper, E., Couturier, S. & Ballivet, M. (1991) Pentameric structure and subunit stoichiometry of a neuronal nicotinic acetylcholine receptor. *Nature*, **350**, 235-238.

Cordero-Erausquin, M., Marubio, L.M., Klink, R. & Changeux, J.P. (2000) Nicotinic receptor function: new perspectives from knockout mice. *Trends in pharmacological sciences*, **21**, 211-217.

Cui, C., Booker, T.K., Allen, R.S., Grady, S.R., Whiteaker, P., Marks, M.J., Salminen, O., Tritto, T., Butt, C.M., Allen, W.R., Stitzel, J.A., McIntosh, J.M., Boulter, J., Collins, A.C. & Heinemann, S.F. (2003) The beta3 nicotinic receptor subunit: a component of alpha-conotoxin MII-binding nicotinic acetylcholine receptors that modulate dopamine release and related behaviors. *The Journal of neuroscience : the official journal of the Society for Neuroscience*, **23**, 11045-11053.

David, R., Ciuraszkiewicz, A., Simeone, X., Orr-Urtreger, A., Papke, R.L., McIntosh, J.M., Huck, S. & Scholze, P. (2010) Biochemical and functional properties of distinct nicotinic acetylcholine receptors in the superior cervical ganglion of mice with targeted deletions of nAChR subunit genes. *The European journal of neuroscience*, **31**, 978-993.

Eng, C.M., Kozak, C.A., Beaudet, A.L. & Zoghbi, H.Y. (1991) Mapping of multiple subunits of the neuronal nicotinic acetylcholine receptor to chromosome 15 in man and chromosome 9 in mouse. *Genomics*, **9**, 278-282.

Fischer, A.H., Jacobson, K.A., Rose, J. & Zeller, R. (2008) Cryosectioning tissues. *CSH protocols*, **2008**, pdb prot4991.

Fowler, C.D., Arends, M.A. & Kenny, P.J. (2008) Subtypes of nicotinic acetylcholine receptors in nicotine reward, dependence, and withdrawal: evidence from genetically modified mice. *Behavioural pharmacology*, **19**, 461-484.

Frahm, S., Slimak, M.A., Ferrarese, L., Santos-Torres, J., Antolin-Fontes, B., Auer, S., Filkin, S., Pons, S., Fontaine, J.F., Tsetlin, V., Maskos, U. & Ibanez-Tallon, I. (2011) Aversion to nicotine is regulated by the balanced activity of beta4 and alpha5 nicotinic receptor subunits in the medial habenula. *Neuron*, **70**, 522-535.

Franceschini, D., Orr-Urtreger, A., Yu, W., Mackey, L.Y., Bond, R.A., Armstrong, D., Patrick, J.W., Beaudet, A.L. & De Biasi, M. (2000) Altered baroreflex responses in alpha7 deficient mice. *Behavioural brain research*, **113**, 3-10.

Gerzanich, V., Wang, F., Kuryatov, A. & Lindstrom, J. (1998) alpha 5 Subunit alters desensitization, pharmacology, Ca++ permeability and Ca++ modulation of human neuronal alpha 3 nicotinic receptors. *The Journal of pharmacology and experimental therapeutics*, **286**, 311-320.

Gotti, C. & Clementi, F. (2004) Neuronal nicotinic receptors: from structure to pathology. *Progress in neurobiology*, **74**, 363-396.

Gotti, C., Clementi, F., Fornari, A., Gaimarri, A., Guiducci, S., Manfredi, I., Moretti, M., Pedrazzi, P., Pucci, L. & Zoli, M. (2009) Structural and functional diversity of native brain neuronal nicotinic receptors. *Biochem Pharmacol*, **78**, 703-711.

Gotti, C., Moretti, M., Gaimarri, A., Zanardi, A., Clementi, F. & Zoli, M. (2007) Heterogeneity and complexity of native brain nicotinic receptors. *Biochem Pharmacol*, **74**, 1102-1111.

Gotti, C., Riganti, L., Vailati, S. & Clementi, F. (2006) Brain neuronal nicotinic receptors as new targets for drug discovery. *Current pharmaceutical design*, **12**, 407-428.

Grady, S.R., Moretti, M., Zoli, M., Marks, M.J., Zanardi, A., Pucci, L., Clementi, F. & Gotti, C. (2009) Rodent habenulo-interpeduncular pathway expresses a large variety of uncommon nAChR subtypes, but only the alpha3beta4* and alpha3beta3beta4* subtypes mediate acetylcholine release. *The Journal of neuroscience : the official journal of the Society for Neuroscience*, **29**, 2272-2282.

Hung, R.J., McKay, J.D., Gaborieau, V., Boffetta, P., Hashibe, M., Zaridze, D., Mukeria, A., Szeszenia-Dabrowska, N., Lissowska, J., Rudnai, P., Fabianova, E., Mates, D., Bencko, V., Foretova, L., Janout, V., Chen, C., Goodman, G., Field, J.K., Liloglou, T., Xinarianos, G., Cassidy, A., McLaughlin, J., Liu, G., Narod, S., Krokan, H.E., Skorpen, F., Elvestad, M.B., Hveem, K., Vatten, L., Linseisen, J.,

Clavel-Chapelon, F., Vineis, P., Bueno-de-Mesquita, H.B., Lund, E., Martinez, C., Bingham, S., Rasmuson, T., Hainaut, P., Riboli, E., Ahrens, W., Benhamou, S., Lagiou, P., Trichopoulos, D., Holcatova, I., Merletti, F., Kjaerheim, K., Agudo, A., Macfarlane, G., Talamini, R., Simonato, L., Lowry, R., Conway, D.I., Znaor, A., Healy, C., Zelenika, D., Boland, A., Delepine, M., Foglio, M., Lechner, D., Matsuda, F., Blanche, H., Gut, I., Heath, S., Lathrop, M. & Brennan, P. (2008) A susceptibility locus for lung cancer maps to nicotinic acetylcholine receptor subunit genes on 15q25. *Nature*, **452**, 633-637.

Hurst, R., Rollema, H. & Bertrand, D. (2013) Nicotinic acetylcholine receptors: from basic science to therapeutics. *Pharmacology & therapeutics*, **137**, 22-54.

Jackson, K.J., Marks, M.J., Vann, R.E., Chen, X., Gamage, T.F., Warner, J.A. & Damaj, M.I. (2010) Role of alpha5 nicotinic acetylcholine receptors in pharmacological and behavioral effects of nicotine in mice. *The Journal of pharmacology and experimental therapeutics*, **334**, 137-146.

Jackson, K.J., Martin, B.R., Changeux, J.P. & Damaj, M.I. (2008) Differential role of nicotinic acetylcholine receptor subunits in physical and affective nicotine withdrawal signs. *The Journal of pharmacology and experimental therapeutics*, **325**, 302-312.

Jensen, A.A., Frolund, B., Liljefors, T. & Krogsgaard-Larsen, P. (2005) Neuronal nicotinic acetylcholine receptors: structural revelations, target identifications, and therapeutic inspirations. *Journal of medicinal chemistry*, **48**, 4705-4745.

Jordan, M., Schallhorn, A. & Wurm, F.M. (1996) Transfecting mammalian cells: optimization of critical parameters affecting calcium-phosphate precipitate formation. *Nucleic acids research*, **24**, 596-601.

Kedmi, M., Beaudet, A.L. & Orr-Urtreger, A. (2004) Mice lacking neuronal nicotinic acetylcholine receptor beta4-subunit and mice lacking both alpha5- and beta4-subunits are highly resistant to nicotine-induced seizures. *Physiological genomics*, **17**, 221-229.

Klemm, W.R. (2004) Habenular and interpeduncularis nuclei: shared components in multiple-function networks. *Medical science monitor : international medical journal of experimental and clinical research*, **10**, RA261-273.

Klink, R., de Kerchove d'Exaerde, A., Zoli, M. & Changeux, J.P. (2001) Molecular and physiological diversity of nicotinic acetylcholine receptors in the midbrain dopaminergic nuclei. *The Journal of neuroscience : the official journal of the Society for Neuroscience*, **21**, 1452-1463.

Kobayashi, Y., Sano, Y., Vannoni, E., Goto, H., Suzuki, H., Oba, A., Kawasaki, H., Kanba, S., Lipp, H.P., Murphy, N.P., Wolfer, D.P. & Itohara, S. (2013) Genetic dissection of medial habenula-interpeduncular nucleus pathway function in mice. *Frontiers in behavioral neuroscience*, **7**, 17.

Krishnaswamy, A. & Cooper, E. (2009) An activity-dependent retrograde signal induces the expression of the high-affinity choline transporter in cholinergic neurons. *Neuron*, **61**, 272-286.

Kuryatov, A., Onksen, J. & Lindstrom, J. (2008) Roles of accessory subunits in alpha4beta2(*) nicotinic receptors. *Molecular pharmacology*, **74**, 132-143.

Leslie, F.M., Mojica, C.Y. & Reynaga, D.D. (2013) Nicotinic receptors in addiction pathways. *Molecular pharmacology*, **83**, 753-758.

Lindstrom, J. (1997) Nicotinic acetylcholine receptors in health and disease. *Molecular neurobiology*, **15**, 193-222.

Lorincz, A. & Nusser, Z. (2008) Specificity of immunoreactions: the importance of testing specificity in each method. *The Journal of neuroscience : the official journal of the Society for Neuroscience*, **28**, 9083-9086.

Luetje, C.W. & Patrick, J. (1991) Both alpha- and beta-subunits contribute to the agonist sensitivity of neuronal nicotinic acetylcholine receptors. *The Journal of neuroscience : the official journal of the Society for Neuroscience*, **11**, 837-845.

Lukas, R.J. & Bencherif, M. (1992) Heterogeneity and regulation of nicotinic acetylcholine receptors. *International review of neurobiology*, **34**, 25-131.

Mao, D., Perry, D.C., Yasuda, R.P., Wolfe, B.B. & Kellar, K.J. (2008) The alpha4beta2alpha5 nicotinic cholinergic receptor in rat brain is resistant to up-regulation by nicotine in vivo. *Journal of neurochemistry*, **104**, 446-456.

Mao, D., Yasuda, R.P., Fan, H., Wolfe, B.B. & Kellar, K.J. (2006) Heterogeneity of nicotinic cholinergic receptors in rat superior cervical and nodose Ganglia. *Molecular pharmacology*, **70**, 1693-1699.

Marubio, L.M., del Mar Arroyo-Jimenez, M., Cordero-Erausquin, M., Lena, C., Le Novere, N., de Kerchove d'Exaerde, A., Huchet, M., Damaj, M.I. & Changeux, J.P. (1999) Reduced antinociception in mice lacking neuronal nicotinic receptor subunits. *Nature*, **398**, 805-810.

Miyazawa, A., Fujiyoshi, Y. & Unwin, N. (2003) Structure and gating mechanism of the acetylcholine receptor pore. *Nature*, **423**, 949-955.

Morel, C., Fattore, L., Pons, S., Hay, Y.A., Marti, F., Lambolez, B., De Biasi, M., Lathrop, M., Fratta, W., Maskos, U. & Faure, P. (2013) Nicotine consumption is regulated by a human polymorphism in dopamine neurons. *Molecular psychiatry*.

Moser, N., Mechawar, N., Jones, I., Gochberg-Sarver, A., Orr-Urtreger, A., Plomann, M., Salas, R., Molles, B., Marubio, L., Roth, U., Maskos, U., Winzer-Serhan, U., Bourgeois, J.P., Le Sourd, A.M., De Biasi, M., Schroder, H., Lindstrom, J., Maelicke, A., Changeux, J.P. & Wevers, A. (2007) Evaluating the suitability of nicotinic acetylcholine receptor antibodies for standard immunodetection procedures. *Journal of neurochemistry*, **102**, 479-492.

Mossier, B., Togel, M., Fuchs, K. & Sieghart, W. (1994) Immunoaffinity purification of gamma-aminobutyric acidA (GABAA) receptors containing gamma 1-subunits. Evidence for the presence of a single type of gamma-subunit in GABAA receptors. *The Journal of biological chemistry*, **269**, 25777-25782.

Nelson, M.E., Wang, F., Kuryatov, A., Choi, C.H., Gerzanich, V. & Lindstrom, J. (2001) Functional properties of human nicotinic AChRs expressed by IMR-32 neuroblastoma cells resemble those of alpha3beta4 AChRs expressed in permanently transfected HEK cells. *The Journal of general physiology*, **118**, 563-582.

Orr-Urtreger, A., Goldner, F.M., Saeki, M., Lorenzo, I., Goldberg, L., De Biasi, M., Dani, J.A., Patrick, J.W. & Beaudet, A.L. (1997) Mice deficient in the alpha7 neuronal nicotinic acetylcholine receptor lack alpha-bungarotoxin binding sites and hippocampal fast nicotinic currents. *The Journal of neuroscience : the official journal of the Society for Neuroscience*, **17**, 9165-9171.

Passetti, F., Dalley, J.W., O'Connell, M.T., Everitt, B.J. & Robbins, T.W. (2000) Increased acetylcholine release in the rat medial prefrontal cortex during performance of a visual attentional task. *The European journal of neuroscience*, **12**, 3051-3058.

Picciotto, M.R., Caldarone, B.J., King, S.L. & Zachariou, V. (2000) Nicotinic receptors in the brain. Links between molecular biology and behavior. *Neuropsychopharmacology : official publication of the American College of Neuropsychopharmacology*, **22**, 451-465.

Picciotto, M.R., Zoli, M., Lena, C., Bessis, A., Lallemand, Y., Le Novere, N., Vincent, P., Pich, E.M., Brulet, P. & Changeux, J.P. (1995) Abnormal avoidance learning in mice lacking functional high-affinity nicotine receptor in the brain. *Nature*, **374**, 65-67.

Purves, D., Snider, W.D. & Voyvodic, J.T. (1988) Trophic regulation of nerve cell morphology and innervation in the autonomic nervous system. *Nature*, **336**, 123-128.

Putz, G., Kristufek, D., Orr-Urtreger, A., Changeux, J.P., Huck, S. & Scholze, P. (2008) Nicotinic acetylcholine receptor-subunit mRNAs in the mouse superior cervical ganglion are regulated by development but not by deletion of distinct subunit genes. *Journal of neuroscience research*, **86**, 972-981.

Ramirez-Latorre, J., Yu, C.R., Qu, X., Perin, F., Karlin, A. & Role, L. (1996) Functional contributions of alpha5 subunit to neuronal acetylcholine receptor channels. *Nature*, **380**, 347-351.

Rassadi, S., Krishnaswamy, A., Pie, B., McConnell, R., Jacob, M.H. & Cooper, E. (2005) A null mutation for the alpha3 nicotinic acetylcholine (ACh) receptor gene abolishes fast synaptic activity in sympathetic ganglia and reveals that ACh output from developing preganglionic terminals is regulated in an activity-dependent retrograde manner. *The Journal of neuroscience : the official journal of the Society for Neuroscience*, **25**, 8555-8566.

Saccone, N.L., Wang, J.C., Breslau, N., Johnson, E.O., Hatsukami, D., Saccone, S.F., Grucza, R.A., Sun, L., Duan, W., Budde, J., Culverhouse, R.C., Fox, L., Hinrichs, A.L., Steinbach, J.H., Wu, M., Rice, J.P., Goate, A.M. & Bierut, L.J. (2009) The CHRNA5-CHRNA3-CHRNB4 nicotinic receptor subunit gene cluster affects risk for nicotine dependence in African-Americans and in European-Americans. *Cancer research*, **69**, 6848-6856.

Salas, R., Orr-Urtreger, A., Broide, R.S., Beaudet, A., Paylor, R. & De Biasi, M. (2003) The nicotinic acetylcholine receptor subunit alpha 5 mediates short-term effects of nicotine in vivo. *Molecular pharmacology*, **63**, 1059-1066.

Salas, R., Pieri, F. & De Biasi, M. (2004) Decreased signs of nicotine withdrawal in mice null for the beta4 nicotinic acetylcholine receptor subunit. *The Journal of neuroscience : the official journal of the Society for Neuroscience*, **24**, 10035-10039.

Salas, R., Sturm, R., Boulter, J. & De Biasi, M. (2009) Nicotinic receptors in the habenulo-interpeduncular system are necessary for nicotine withdrawal in mice. *The Journal of neuroscience : the official journal of the Society for Neuroscience*, **29**, 3014-3018.

Schneider Gasser, E.M., Straub, C.J., Panzanelli, P., Weinmann, O., Sassoe-Pognetto, M. & Fritschy, J.M. (2006) Immunofluorescence in brain sections: simultaneous detection of presynaptic and postsynaptic proteins in identified neurons. *Nature protocols*, **1**, 1887-1897.

Scholze, P., Ciuraszkiewicz, A., Groessl, F., Orr-Urtreger, A., McIntosh, J.M. & Huck, S. (2011) alpha4beta2 nicotinic acetylcholine receptors in the early postnatal mouse superior cervical ganglion. *Developmental neurobiology*, **71**, 390-399.

Scholze, P., Koth, G., Orr-Urtreger, A. & Huck, S. (2012) Subunit composition of alpha5-containing nicotinic receptors in the rodent habenula. *Journal of neurochemistry*, **121**, 551-560.

Semenova, S., Contet, C., Roberts, A.J. & Markou, A. (2012) Mice lacking the beta4 subunit of the nicotinic acetylcholine receptor show memory deficits, altered anxiety- and depression-like behavior, and diminished nicotine-induced analgesia. *Nicotine & tobacco research : official journal of the Society for Research on Nicotine and Tobacco*, **14**, 1346-1355.

Suarez, S.V., Amadon, A., Giacomini, E., Wiklund, A., Changeux, J.P., Le Bihan, D. & Granon, S. (2009) Brain activation by short-term nicotine exposure in anesthetized wild-type and beta2-nicotinic receptors knockout mice: a BOLD fMRI study. *Psychopharmacology*, **202**, 599-610.

Toyoshima, C. & Unwin, N. (1988) Ion channel of acetylcholine receptor reconstructed from images of postsynaptic membranes. *Nature*, **336**, 247-250.

Unwin, N. (1998) The nicotinic acetylcholine receptor of the Torpedo electric ray. *Journal of structural biology*, **121**, 181-190.

Unwin, N. (2005) Refined structure of the nicotinic acetylcholine receptor at 4A resolution. *Journal of molecular biology*, **346**, 967-989.

Vetter, D.E., Liberman, M.C., Mann, J., Barhanin, J., Boulter, J., Brown, M.C., Saffiote-Kolman, J., Heinemann, S.F. & Elgoyhen, A.B. (1999) Role of alpha9 nicotinic ACh receptor subunits in the development and function of cochlear efferent innervation. *Neuron*, **23**, 93-103.

Vincler, M. & Eisenach, J.C. (2004) Plasticity of spinal nicotinic acetylcholine receptors following spinal nerve ligation. *Neuroscience research*, **48**, 139-145.

Vincler, M.A. & Eisenach, J.C. (2005) Knock down of the alpha 5 nicotinic acetylcholine receptor in spinal nerve-ligated rats alleviates mechanical allodynia. *Pharmacology, biochemistry, and behavior*, **80**, 135-143.

Wang, F., Gerzanich, V., Wells, G.B., Anand, R., Peng, X., Keyser, K. & Lindstrom, J. (1996) Assembly of human neuronal nicotinic receptor alpha5 subunits with alpha3, beta2, and beta4 subunits. *The Journal of biological chemistry*, **271**, 17656-17665.

Wang, J.C., Cruchaga, C., Saccone, N.L., Bertelsen, S., Liu, P., Budde, J.P., Duan, W., Fox, L., Grucza, R.A., Kern, J., Mayo, K., Reyes, O., Rice, J., Saccone, S.F., Spiegel, N., Steinbach, J.H., Stitzel, J.A., Anderson, M.W., You, M., Stevens, V.L., Bierut, L.J., Goate, A.M., collaborators, C. & collaborators, G. (2009) Risk for nicotine dependence and lung cancer is conferred by mRNA expression levels and amino acid change in CHRNA5. *Human molecular genetics*, **18**, 3125-3135.

Wang, N., Orr-Urtreger, A., Chapman, J., Rabinowitz, R., Nachman, R. & Korczyn, A.D. (2002) Autonomic function in mice lacking alpha5 neuronal nicotinic acetylcholine receptor subunit. *The Journal of physiology*, **542**, 347-354.

Wang, Y., Broderick, P., Matakidou, A., Eisen, T. & Houlston, R.S. (2010) Role of 5p15.33 (TERT-CLPTM1L), 6p21.33 and 15q25.1 (CHRNA5-CHRNA3) variation and lung cancer risk in never-smokers. *Carcinogenesis*, **31**, 234-238.

Watanabe, M., Fukaya, M., Sakimura, K., Manabe, T., Mishina, M. & Inoue, Y. (1998) Selective scarcity of NMDA receptor channel subunits in the stratum lucidum (mossy fibre-recipient layer) of the mouse hippocampal CA3 subfield. *The European journal of neuroscience*, **10**, 478-487.

Wessler, I., Kirkpatrick, C.J. & Racke, K. (1999) The cholinergic 'pitfall': acetylcholine, a universal cell molecule in biological systems, including humans. *Clinical and experimental pharmacology & physiology*, **26**, 198-205.

Wright, L.L. & Smolen, A.J. (1987) The role of neuron death in the development of the gender difference in the number of neurons in the rat superior cervical ganglion. *International journal of developmental neuroscience : the official journal of the International Society for Developmental Neuroscience*, **5**, 305-311.

Xanthos., D.N., Beiersdorf., J.W., Thrun., A., Ianosi., B., Orr-Urtreger., A., Huck., S. & Scholze., P. (2014) Role of α5-containing nicotinic receptors in neuropathic pain and response to

nicotine. *Neuropharmacology*.

Xu, W., Gelber, S., Orr-Urtreger, A., Armstrong, D., Lewis, R.A., Ou, C.N., Patrick, J., Role, L., De Biasi, M. & Beaudet, A.L. (1999a) Megacystis, mydriasis, and ion channel defect in mice lacking the alpha3 neuronal nicotinic acetylcholine receptor. *Proceedings of the National Academy of Sciences of the United States of America*, **96**, 5746-5751.

Xu, W., Orr-Urtreger, A., Nigro, F., Gelber, S., Sutcliffe, C.B., Armstrong, D., Patrick, J.W., Role, L.W., Beaudet, A.L. & De Biasi, M. (1999b) Multiorgan autonomic dysfunction in mice lacking the beta2 and the beta4 subunits of neuronal nicotinic acetylcholine receptors. *The Journal of neuroscience : the official journal of the Society for Neuroscience*, **19**, 9298-9305.

Yang, L., Zhang, F.X., Huang, F., Lu, Y.J., Li, G.D., Bao, L., Xiao, H.S. & Zhang, X. (2004) Peripheral nerve injury induces trans-synaptic modification of channels, receptors and signal pathways in rat dorsal spinal cord. *The European journal of neuroscience*, **19**, 871-883.

Young, H.S., Herbette, L.G. & Skita, V. (2003) Alpha-bungarotoxin binding to acetylcholine receptor membranes studied by low angle X-ray diffraction. *Biophysical journal*, **85**, 943-953.

Young, T., Wittenauer, S., Parker, R. & Vincler, M. (2008) Peripheral nerve injury alters spinal nicotinic acetylcholine receptor pharmacology. *European journal of pharmacology*, **590**, 163-169.

6 Curriculum Vitae

Christoph Zlabinger,

born on April 21st, 1985 as the son of Christine and Alois Zlabinger.

Education

2005 - 2015 Study of molecular biology

University of Vienna, 1010 Wien

Focus on neurosciences and structural biology

Publications:

Nicotinic acetylcholine receptors control acetylcholine and noradrenaline release in the rodent habenulo-interpeduncular complex, Beiranvand et al., British Journal of Pharmacology, 2014, **171** 5209–5224
(http://onlinelibrary.wiley.com/doi/10.1111/bph.12841/abstract)

2004 - 2005 Military service

Dabsch-Kaserne, 2100 Korneuburg

Serving as a medic

1999 - 2004 Technical secondary school

HTL TGM, 1200 Wien

Focus on technical computer sciences

1999 - 2004 Secondary school

BG/BRG, 2000 Stockerau